2016 Fall

"Phase Transformation *in* Materials"

10.24.2016

Eun Soo Park

Office: 33-313
Telephone: 880-7221
Email: espark@snu.ac.kr
Office hours: by an appointment

Summary for previous class

- **Thermally Activated Migration of Grain Boundaries:**

  Metastable equilibrium of grain boundary (Balances of 1) boundary E + 2) surface tension)

  → real curvature (ΔP → ΔG: Gibbs Thomson Eq.) → $F = 2\gamma/r = \Delta G/V_m$ (by curvature)

  (Pulling force per unit area of boundary)

  → Grain coarsening at high T annealing

- **Kinetics of Grain Growth**

  - Grain boundary migration (v) by thermally activated atomic jump

Boundary velocity $$v = \frac{A_2 n_1 v_1 V_m^{\,2}}{N_a RT} \exp\left(-\frac{\Delta G^a}{RT}\right)\frac{\Delta G}{V_m}$$

$v \sim \Delta G/V_m$ driving force

→ $F = \Delta G/V_m$

M : mobility = velocity under unit driving force ~ exp (-1/T)

rate of grain growth $d\underline{D}/dt \sim 1/\underline{D}$, exponentially increase with T

→ $\underline{D} = k't^n$

(Experimental: n << 1/2, ½ at pure metals or high Temp.)

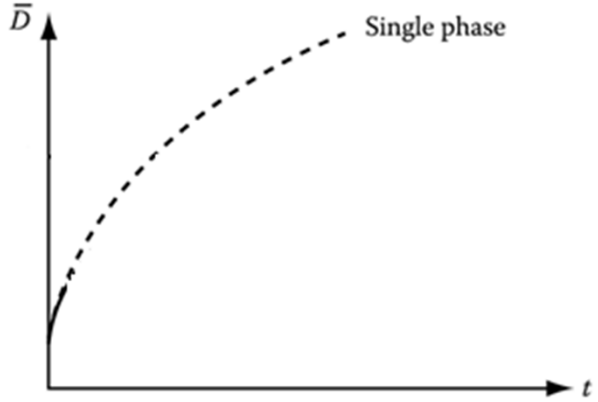

Normal Grain Growth

- Grain boundary moves to reduce area and total energy
- Large grain grow, small grains shrink
- Average grain size increases
- Little change of size distribution

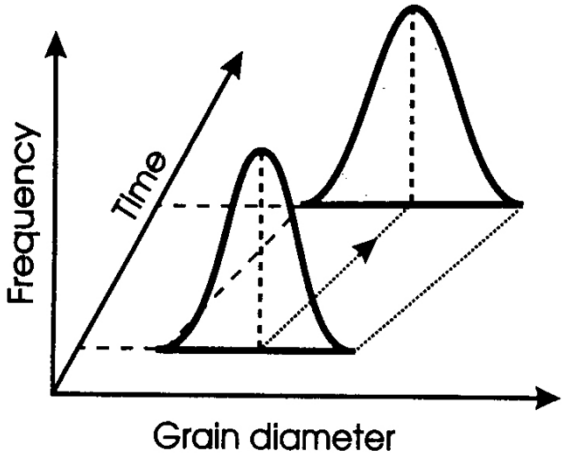

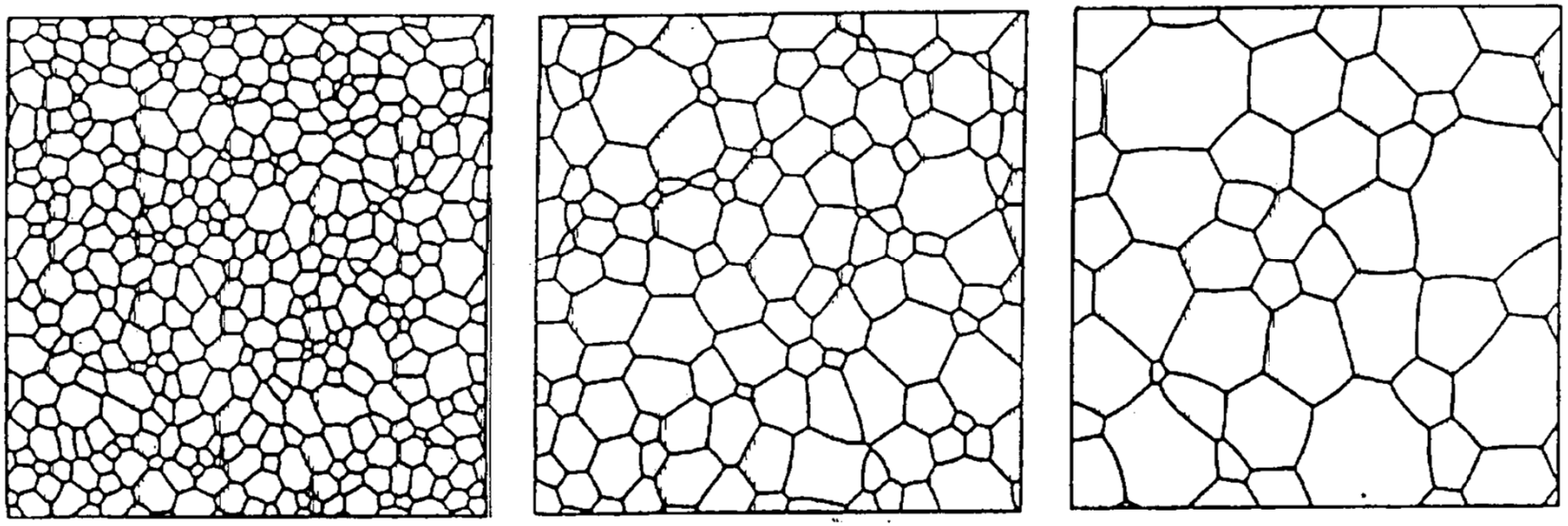

Ref. Hillert ACTA Mater. 13 227 (1965)

Considering factors of G.B. growth

(a) Impurity (solute) drag

(b) Pinning particle

(c) 2^{nd} phases

(d) Anisotropic σ, M

(e) Strain energy

(f) Free surface

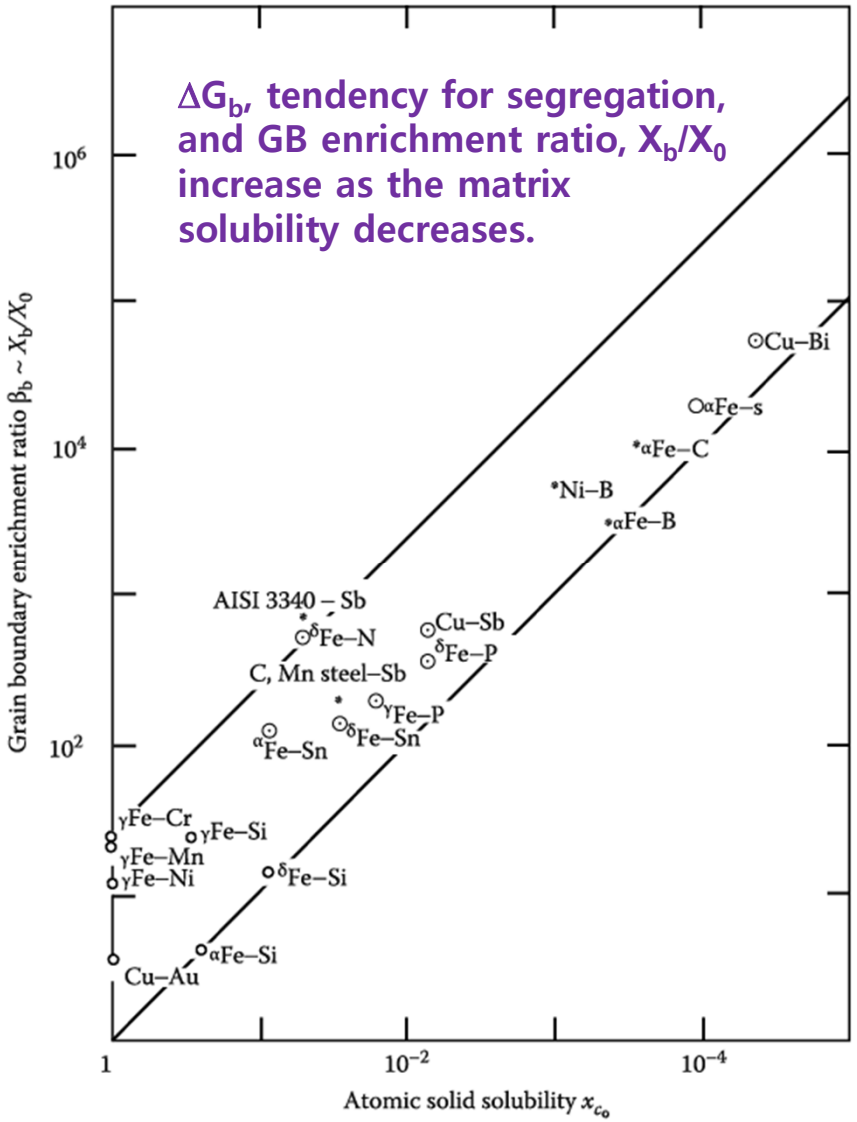

<Increasing GB enrichment with decreasing solid solubility in a range of system>

(a) Impurity (solute) drag

* Solute drag effect

In general,
G_b (grain boundary E) and mobility of pure metal decreases on alloying.

~Impurities tend to stay at the GB.

Generally, ΔG_b, tendency of segregation, increases as the matrix solubility decreases.

$$X_b = X_0 \exp \frac{\Delta G_b}{RT}$$

X_b/X_0: GB enrichment ratio

- Decreases as temp. increases, i.e., the solute "evaporates" into the matrix

Low T or ΔG_b ⇧ X_b ⇧ Mobility of G.B. ⇩

→ Alloying elements affects mobility of G.B.

X_0 : matrix solute concentration/ X_b : boundary solute concentration

ΔG_b : free energy reduced when one mole of solute is moved to GB from matrix.

(ΔG_b) → The high mobility of special boundaries can possibly be attributed to a low solute drag on account of the relatively more close-packed structure of the special boundaries.

(b) Pinning particle or (c) 2nd phases

Schematic diagram illustrating the possible interactions of second phase particles and migrating grain boundaries.

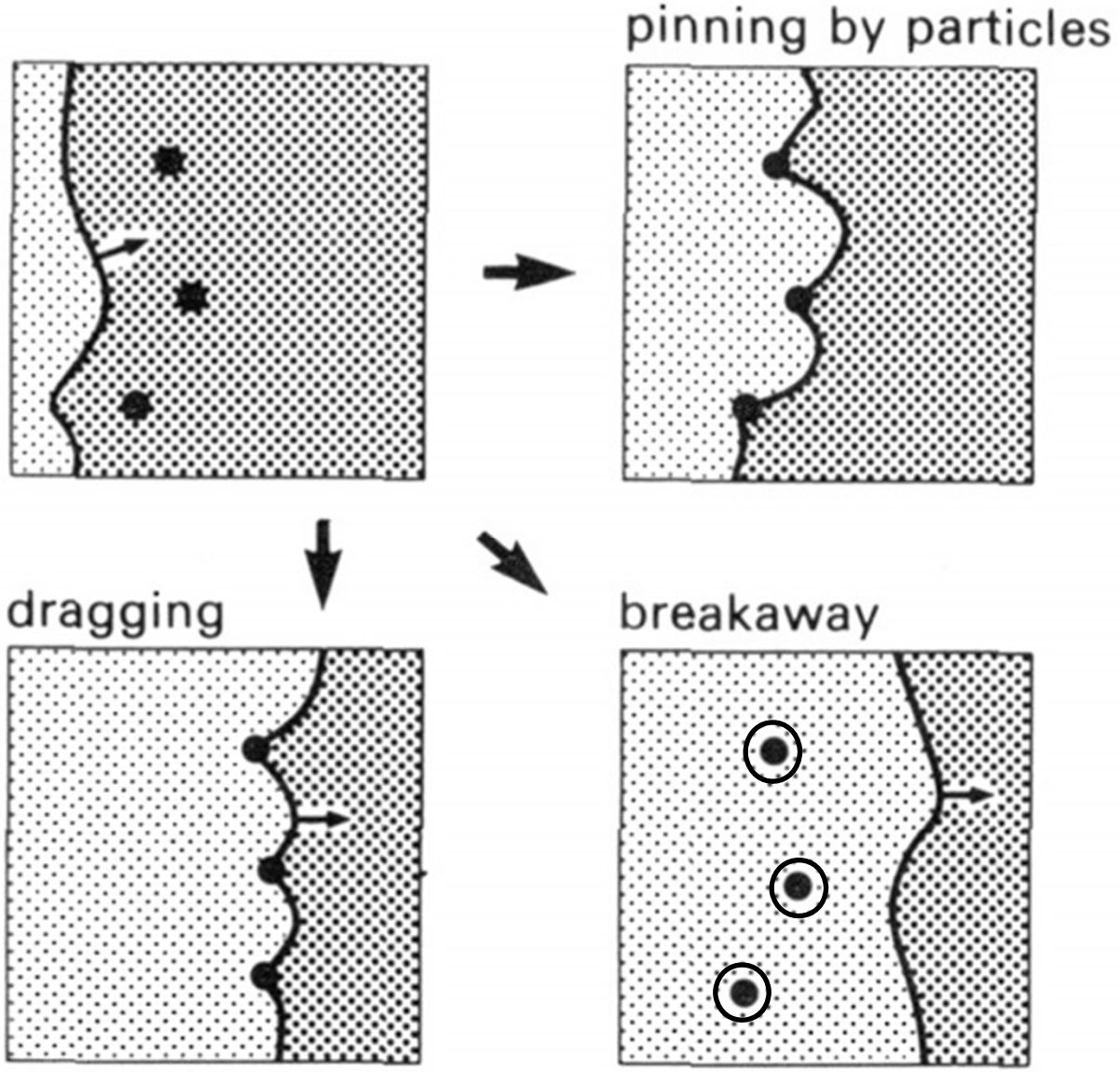

Interaction with particles

Zener Pinning

$$P = \frac{3f_v}{2\pi r^2} \cdot \pi r \gamma = \frac{3f_v \gamma}{2r}$$

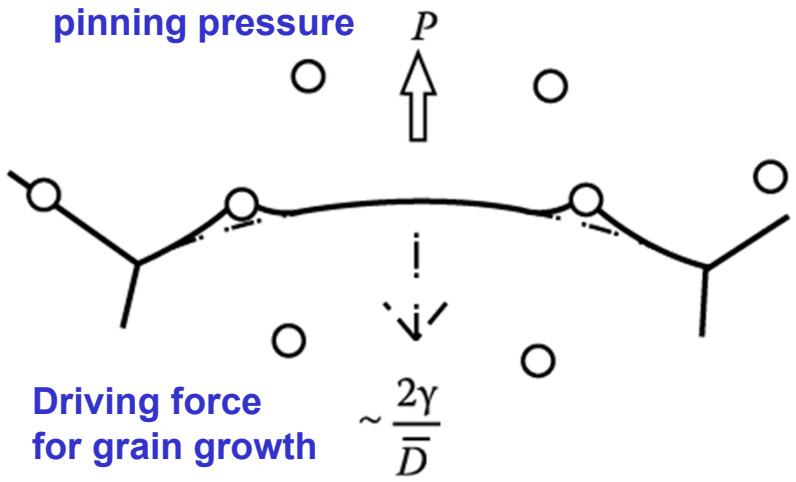

→ F = 2γ/r = ΔG/V_m (by curvature)

This force will oppose the driving force for grain growth, $2\gamma/\bar{D}$.

$$\frac{2\gamma}{\bar{D}} = \frac{3f_v\gamma}{2r} \rightarrow \bar{D}_{max} = \frac{4r}{3f_v}$$

Driving force will be insufficient to overcome the drag of the particles and grain growth stagnates.

For fine grain size
→ a large volume fraction of very small particles

* Effect of second-phase particles on grain growth

$$\bar{D}_{max} = \frac{4r}{3f_v}$$

: Stabilization of a fine grain size during heating at high temp. → large volume fraction (f ↑) of very small particles (r ↓).

$$\bar{D}_{max} = \frac{4r}{3f_v} \downarrow$$

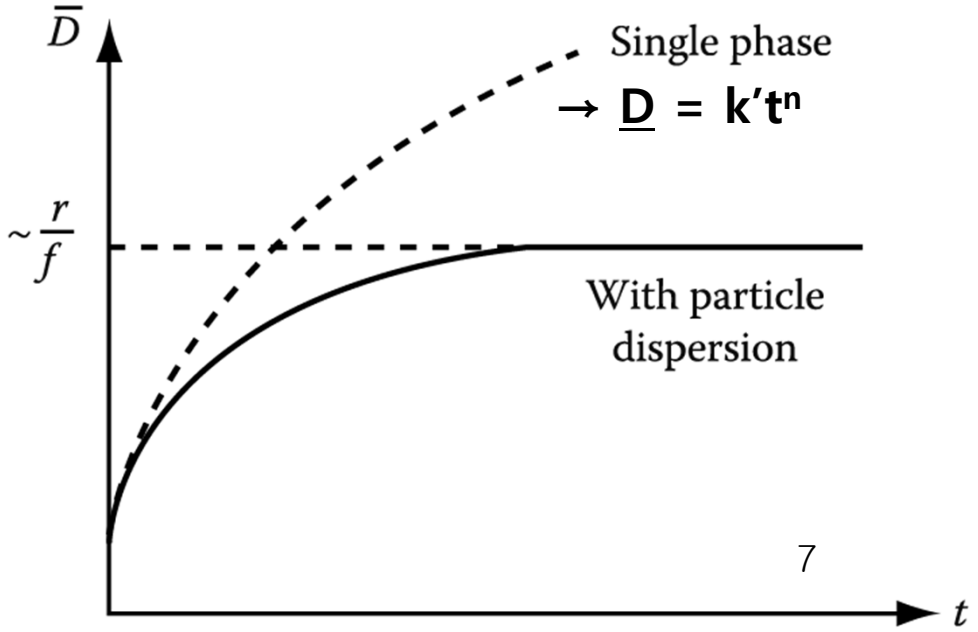

Abnormal Grain Growth

(high mobility of special GBs → development of recrystallization textures)

❑ **Discontinuous grain growth of a few selected grains**

- Local breaking of pinning by precipitates
- Anisotropy of grain boundary mobility
- Anisotropy of surface & grain boundary energy
- Selective segregation of impurity atoms
- Inhomogeneity of strain energy

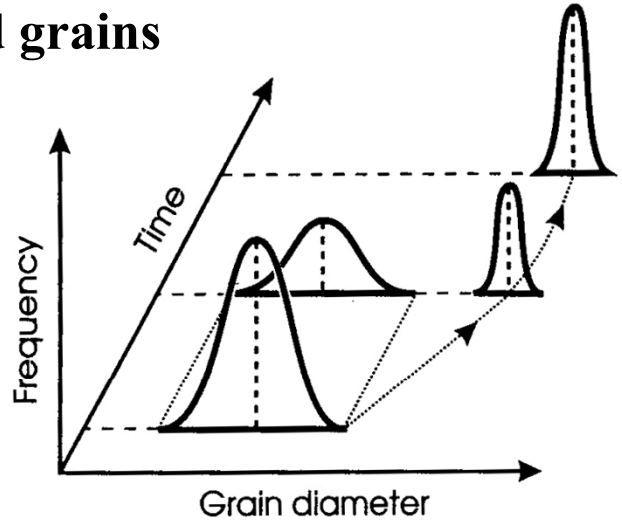

❑ **Bimodal Size distribution**

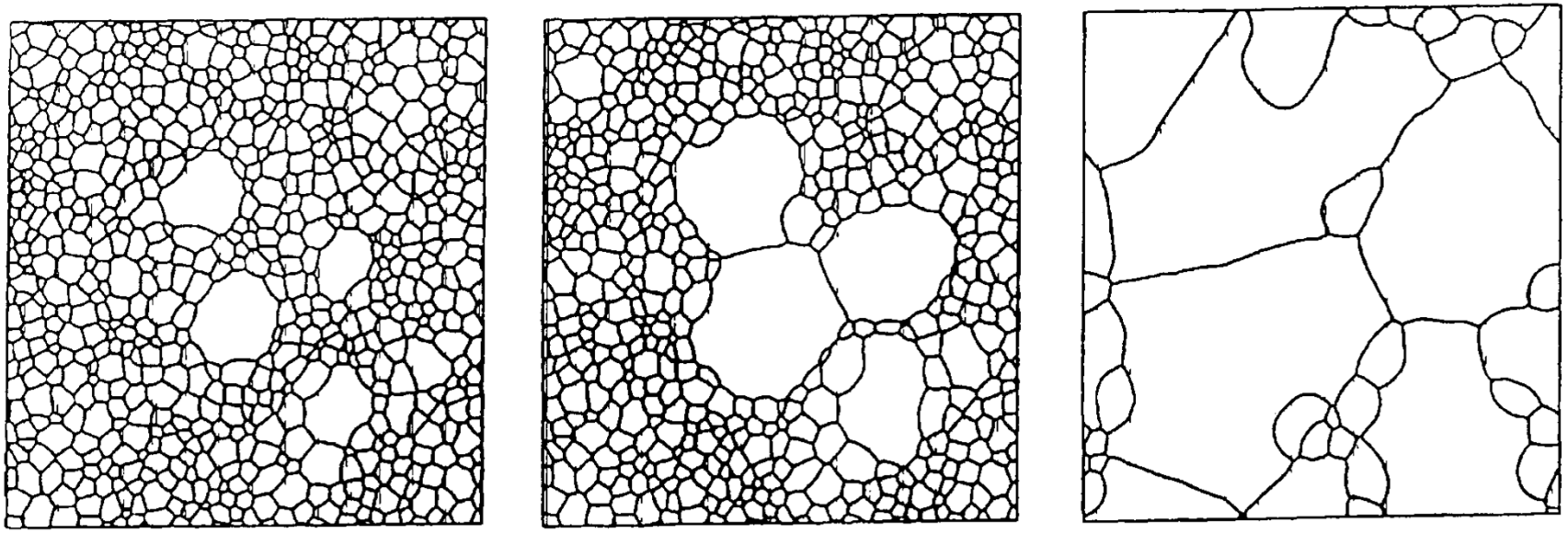

- **Grain Growth**

  - Normal grain growth ⟺ Abnormal grain growth

    (high mobility of special GBs
    → development of recrystallization textures)

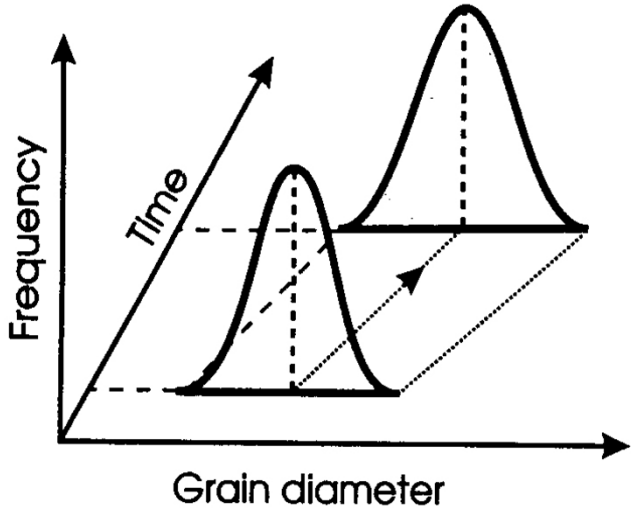

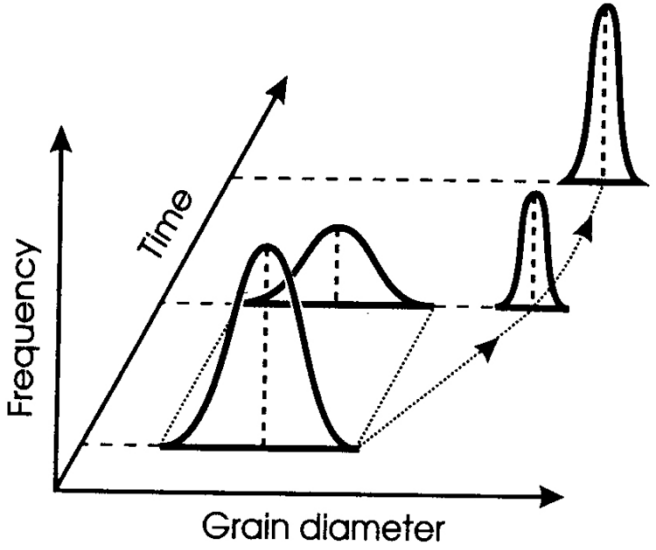

< Bimodal Size distribution >

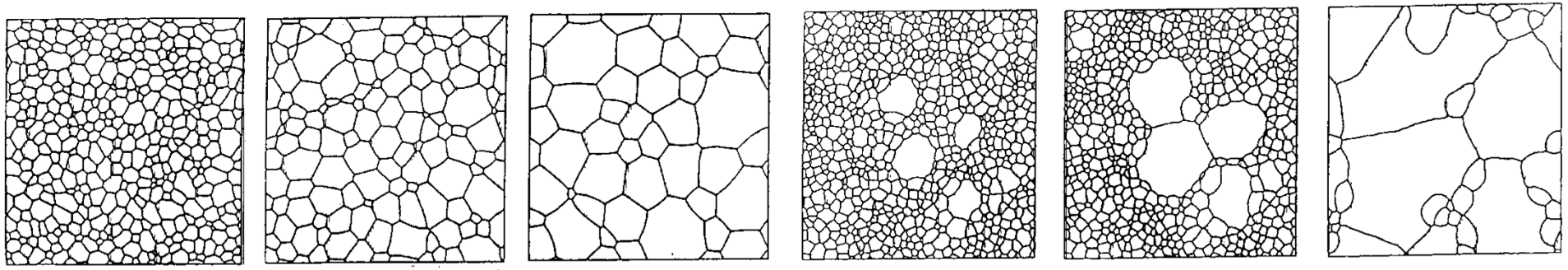

Contents for today's class

- **Interphase Interfaces in Solid (α/β)**

  - Types of interphase interfaces in solid (α/β)

  - Second-Phase Shape

    $$\sum A_i \gamma_i + \Delta G_S = minimum$$

    - Interface Energy Effects
      - Coherent / Semi-coherent / incoherent
    - Misfit Strain Effects

  - Coherency Loss

  - Glissil Interfaces ⟺ Solid/Liquid Interfaces

- **Interface migration**

  - Interface controlled growth ⟺ Diffusion controlled growth

Q: What kind of interphase interfaces in solid (α/β) exist?

= coherent/ semi-coherent / incoherent/ complex semi-coherent

→ different interfacial free energy, γ

3.4 Interphase Interfaces in Solids

Interphase boundary
- different two phases : different crystal structure
different composition

{ **coherent,**
semicoherent
incoherent

3.4.1 Coherent interfaces

Disregarding chemical species, if the interfacial plane has the same atomic configuration in both phases,

Perfect atomic matching at interface

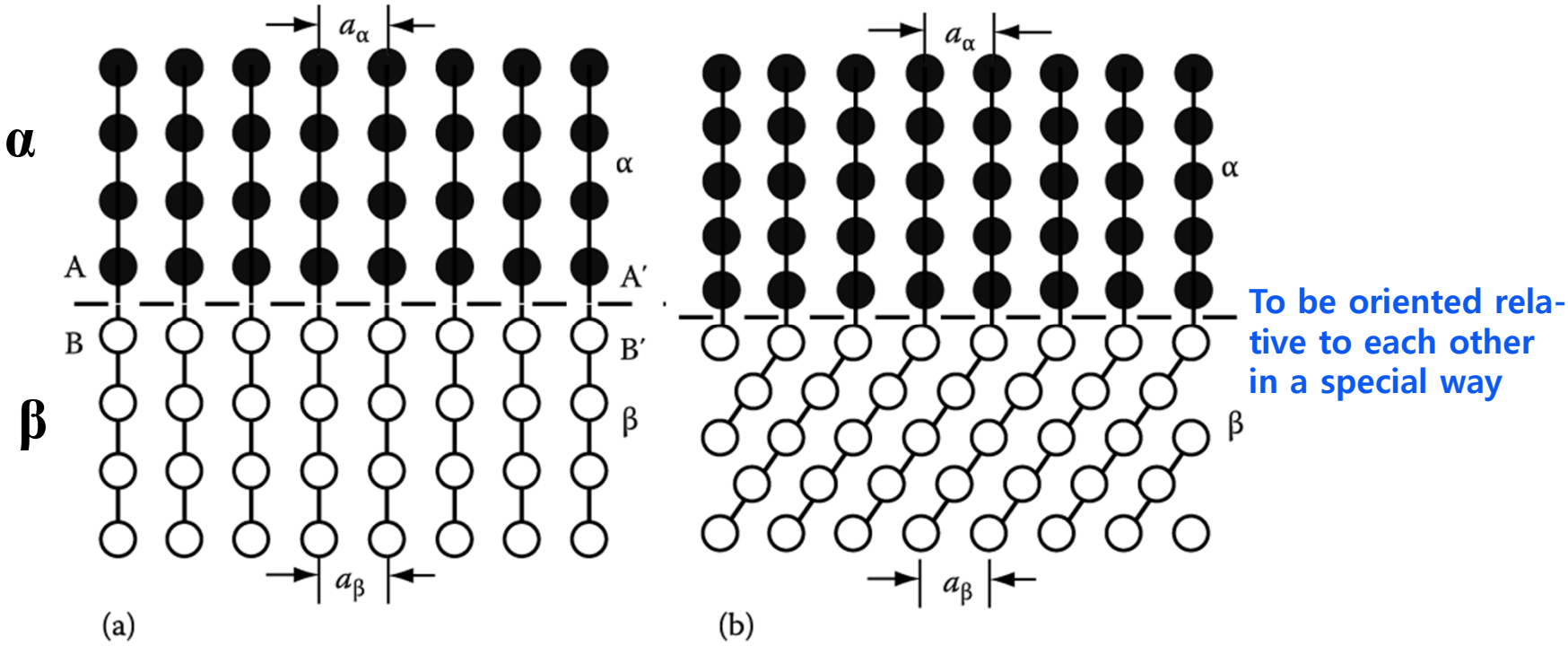

To be oriented relative to each other in a special way

Fig. 3.32 Strain-free coherent interfaces. (a) Each crystal has a different chemical composition but the same crystal structure. (b) The two phases have different lattices

3.4.1 Coherent interfaces

Which plane and direction will be coherent between FCC and HCP?

: **Interphase interface will make lowest energy and thereby the lowest nucleation barrier**

ex) hcp silicon-rich κ phase in fcc copper-rich α matrix of Cu-Si alloy

→ the same atomic configuration
& interatomic distance

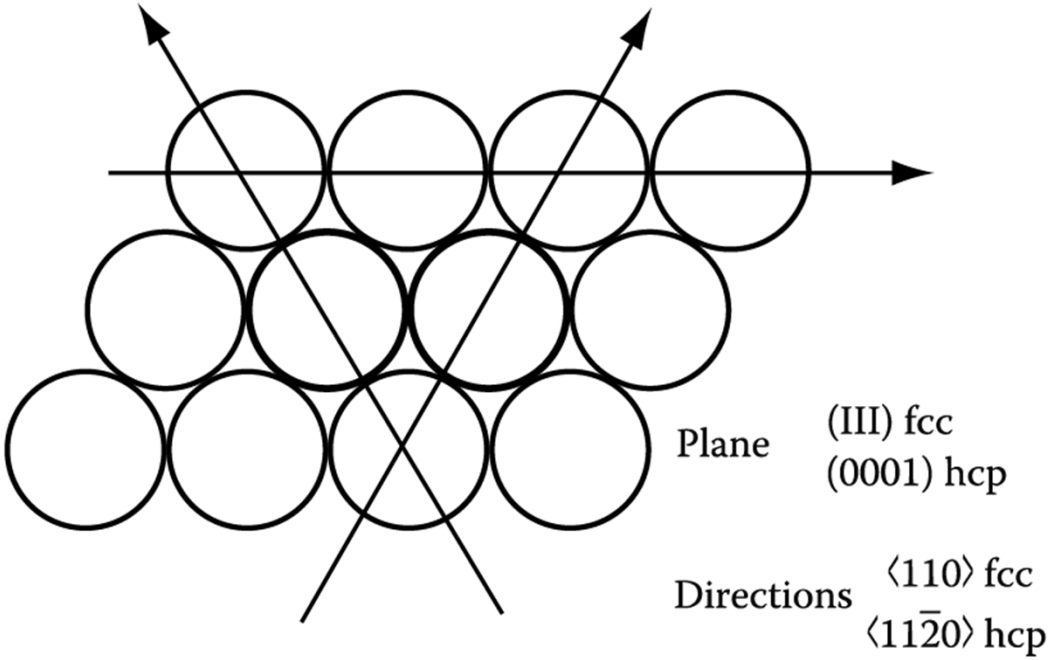

Fig. 3.33 **The close-packed plane and directions in fcc and hcp structures**.

→ Orientation relation

Cu $(111)_\alpha // (0001)_\kappa$ Si

$[\bar{1}10]_\alpha // [11\bar{2}0]_\kappa$

$\gamma_{\alpha\text{-}\kappa}$ of Cu-Si ~ 1 mJm^{-2}

In general,
γ (coherent) ~ 200 mJm^{-2}

$\gamma_{coherent} = \gamma_{structure} + \gamma_{chemical}$

$= \gamma_{chemical}$

γ (coherent) = γ_{ch}

hcp/ fcc interface: only one plane that can form a coherent interface

When the atomic spacing in the interface is not identical between the adjacent phase, what would happen?

Possible to maintain coherency by straining one or both crystal lattices.

→ lattice distortion

→ Coherency strain

→ strain energy

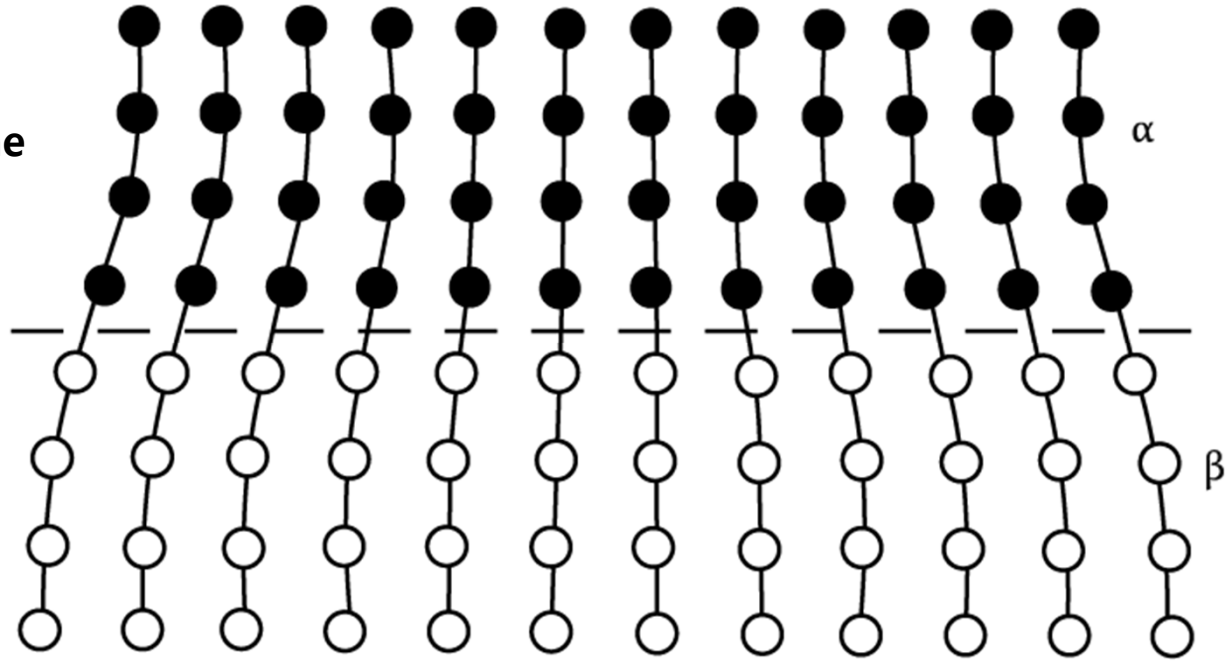

Fig. 3.34 A coherent interface with slight mismatch leads to coherency strains in the adjoining lattices.

The strains associated with a coherent interface raise the total energy of the system.

How can this coherent strain can be reduced?

If coherency strain energy is sufficiently large, → "misfit dislocations"

→ semi-coherent interface

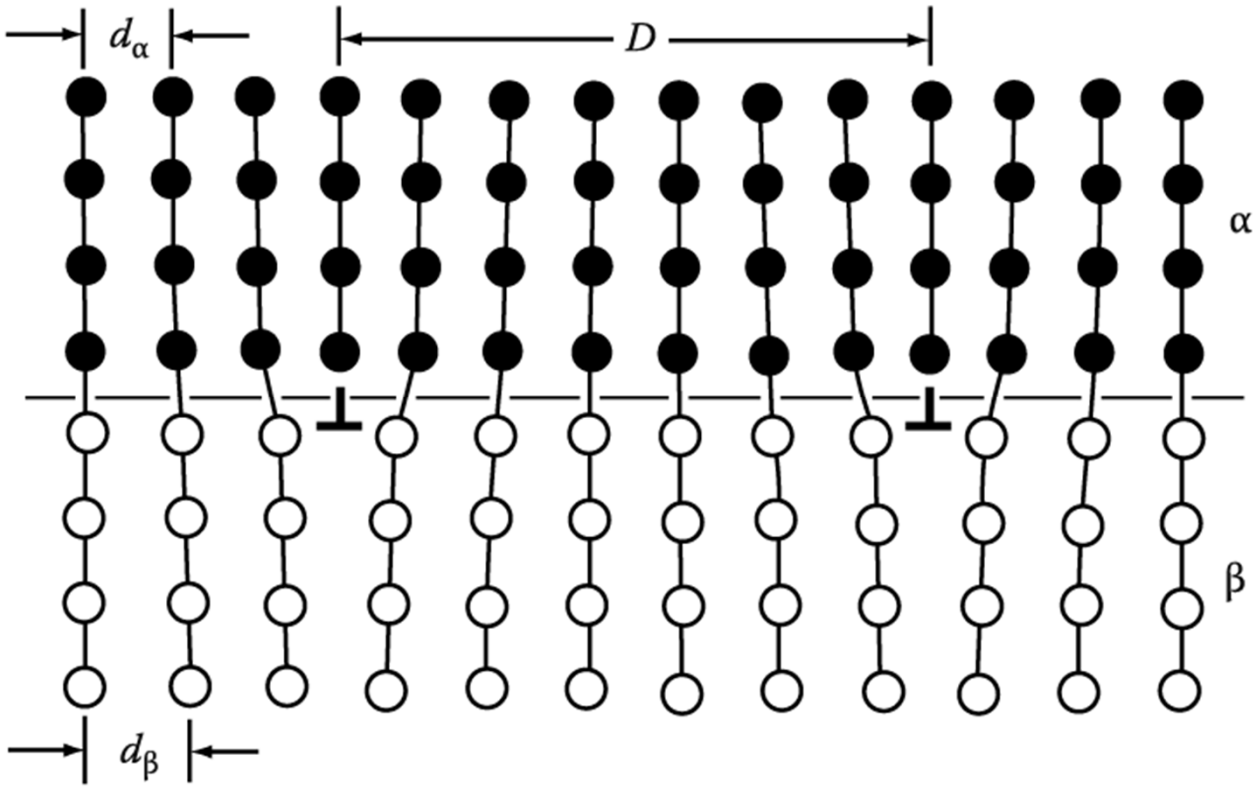

Misfit between the two lattices

$$\delta = \frac{d_\beta - d_\alpha}{d_\alpha}$$

δ~ small,

$$D = \frac{b}{\delta}$$

δ: misfit (disregistry)

b: Burgers vector of disl.

[$b=(d_\alpha + d_\beta)/2$]

Fig. 3.35 A semi-coherent interface. The misfit parallel to the interface is accommodated by a series of edge dislocations.

(2) Semicoherent interfaces

$d_\alpha < d_\beta$

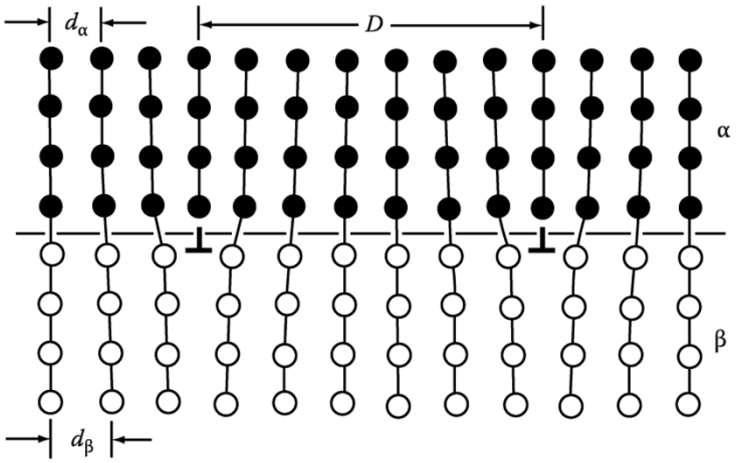

$\delta = (d_\beta - d_\alpha)/ d_\alpha$: misfit

→ D vs. δ vs. n

$(n+1)\, d_\alpha = n\, d_\beta = D$

$\delta = (d_\beta/ d_\alpha) - 1,\ (d_\beta/ d_\alpha) = 1 + 1/n = 1 + \delta$

→ $\delta = 1/n$

$D = d_\beta / \delta \approx b / \delta \quad [b=(d_\alpha + d_\beta)/2]$

δ~ small,

Burgers vector of dislocation

$$\gamma(semicoherent) = \gamma_{ch} + \gamma_{st}$$

γ_{st} → due to **structural distortions** caused by the misfit dislocations

$$\gamma_{st} \propto \delta \text{ for small } \delta$$

In general,
γ (semicoherent) ~ 200~500 mJm^{-2}

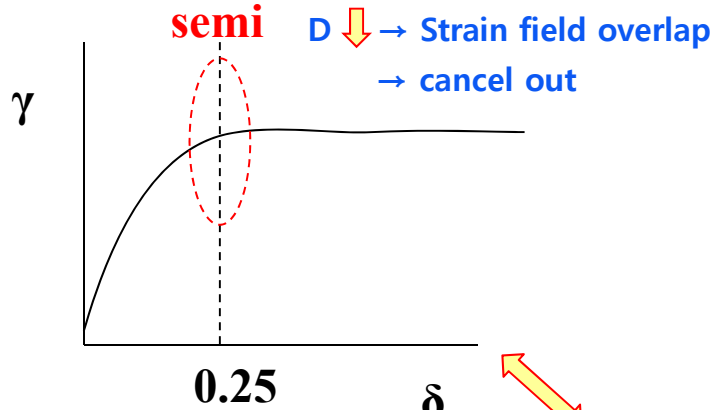

1 dislocation per 4 lattices
n=4

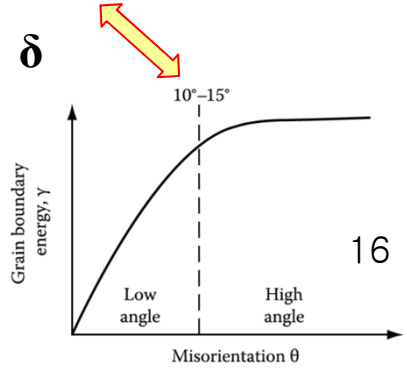

3) Incoherent Interfaces ~ high angle grain boudnary

1) δ > 0.25 No possibility of good matching across the interface

2) different crystal structure (in general)

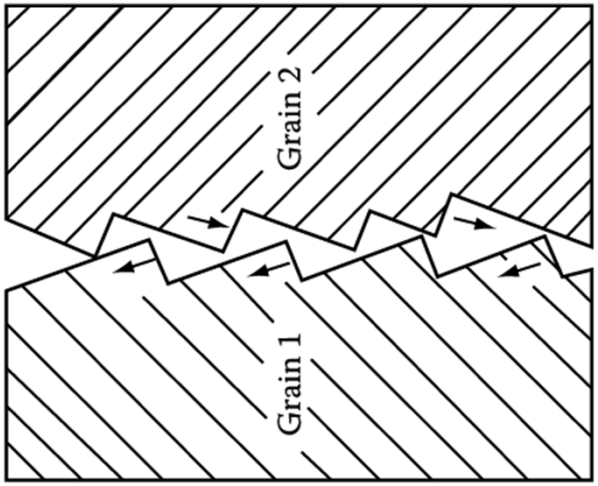

In general,
γ (incoherent) ~ 500~1000 mJm^{-2}

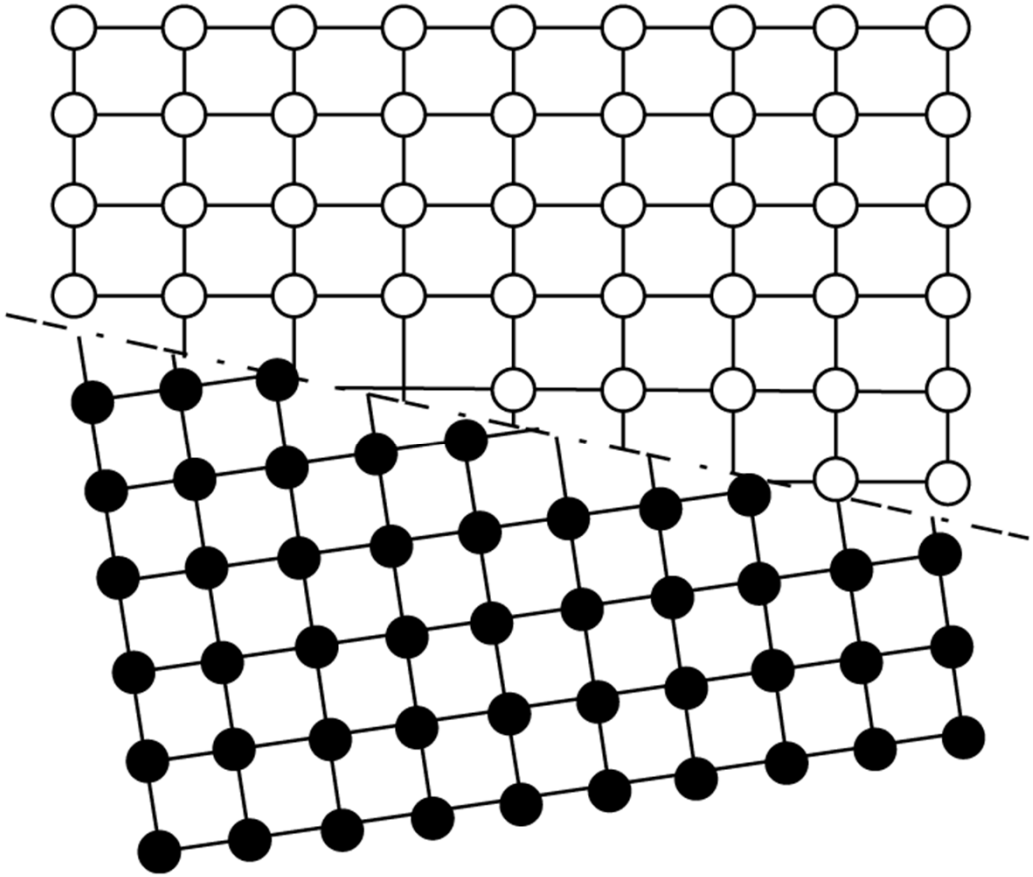

incoherent

Fig. 3.37 An incoherent interface.

4) Complex Semicoherent Interfaces

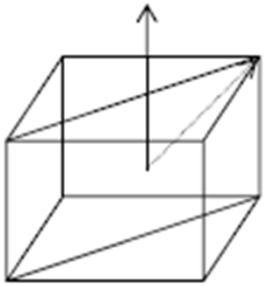

a_α=2.87

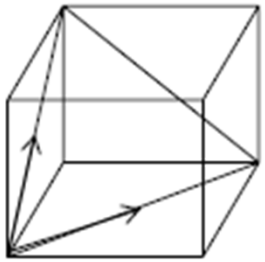

a_γ=3.57

If bcc α is precipitated from fcc γ, which interface is expected?

Which orientation would make the lowest interface energy?

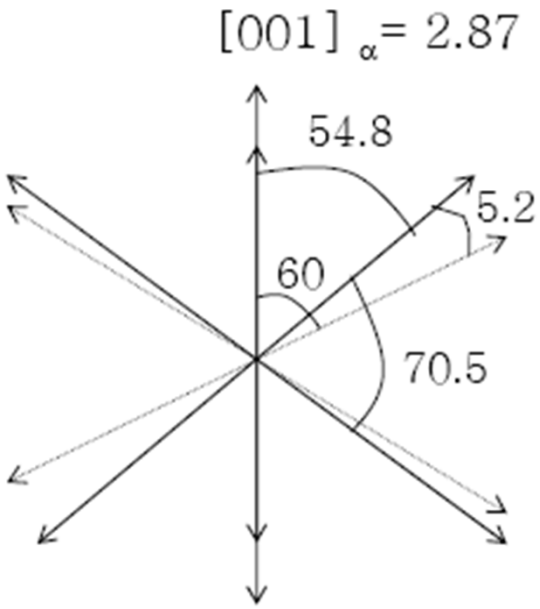

For fcc and bcc crystals ~ closest-pack planes in each phase almost parallel to each other

Nishiyama-Wasserman (N-W) Relationship

$$(110)_{bcc} // (111)_{fcc}, \quad [001]_{bcc} // [\bar{1}01]_{fcc}$$

Kurdjumov-Sachs (K-S) Relationships

$$(110)_{bcc} // (111)_{fcc}, \quad [1\bar{1}1]_{bcc} // [0\bar{1}1]_{fcc}$$

(The only difference between these two is a rotation in the closest-packed planes of 5.26°.)

Complex Semicoherent Interfaces

Semicoherent interface observed at boundaries formed by low-index planes.

(atom pattern and spacing are almost equal.)

N-W relationship

Good fit is restricted to small diamond-shaped areas that only contain ~8% of the orientation relationship.

A similar situation can be shown to exist for the K-S orientation relationship.

⇨ **But,**
impossible to form a large interfaces
→ Incoherent interface

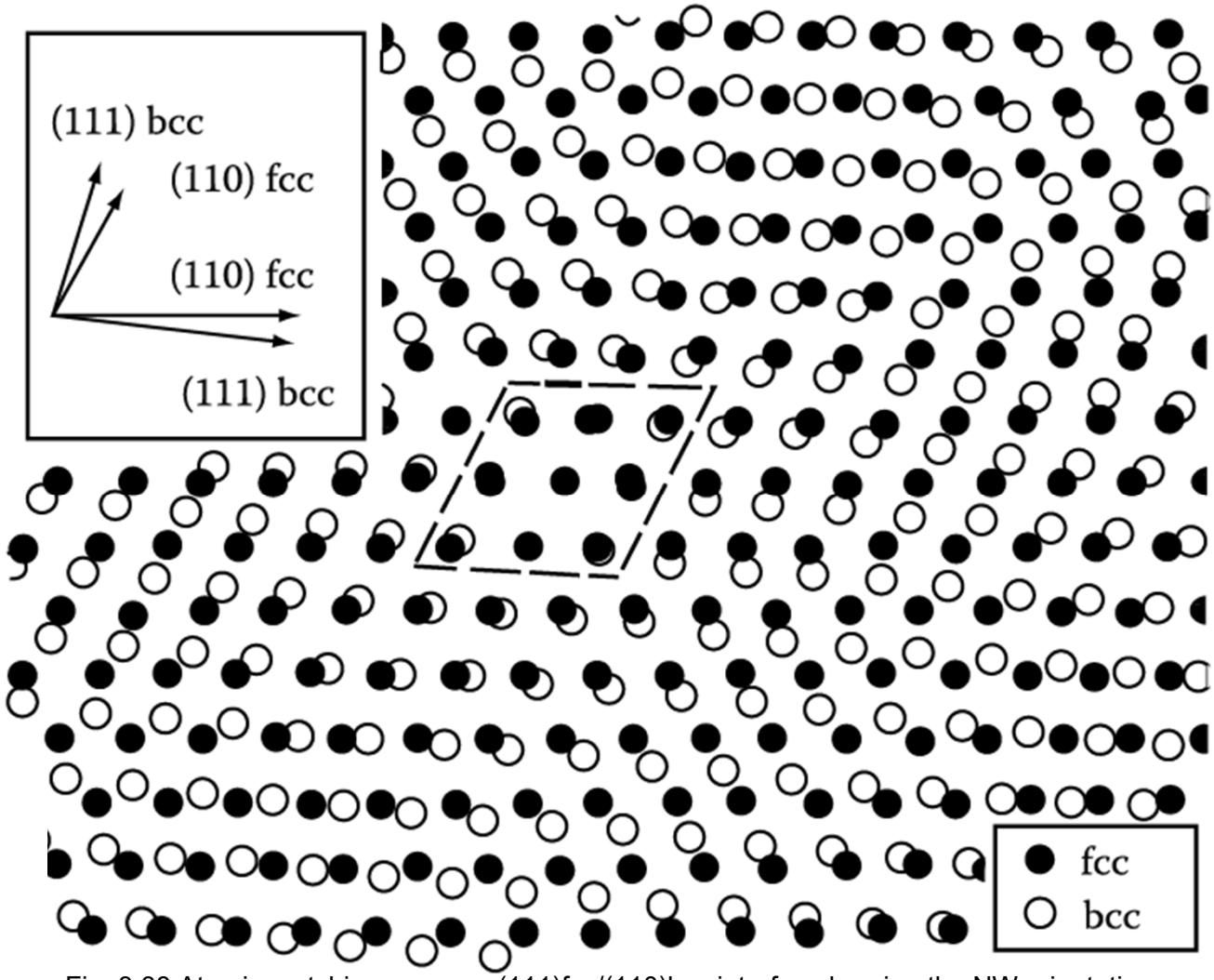

Fig. 3.38 Atomic matching across a (111)fcc/(110)bcc interface bearing the NW orientation relationship for lattice parameters closely corresponding to the case of fcc and bcc iron.

Complex Semicoherent Interfaces

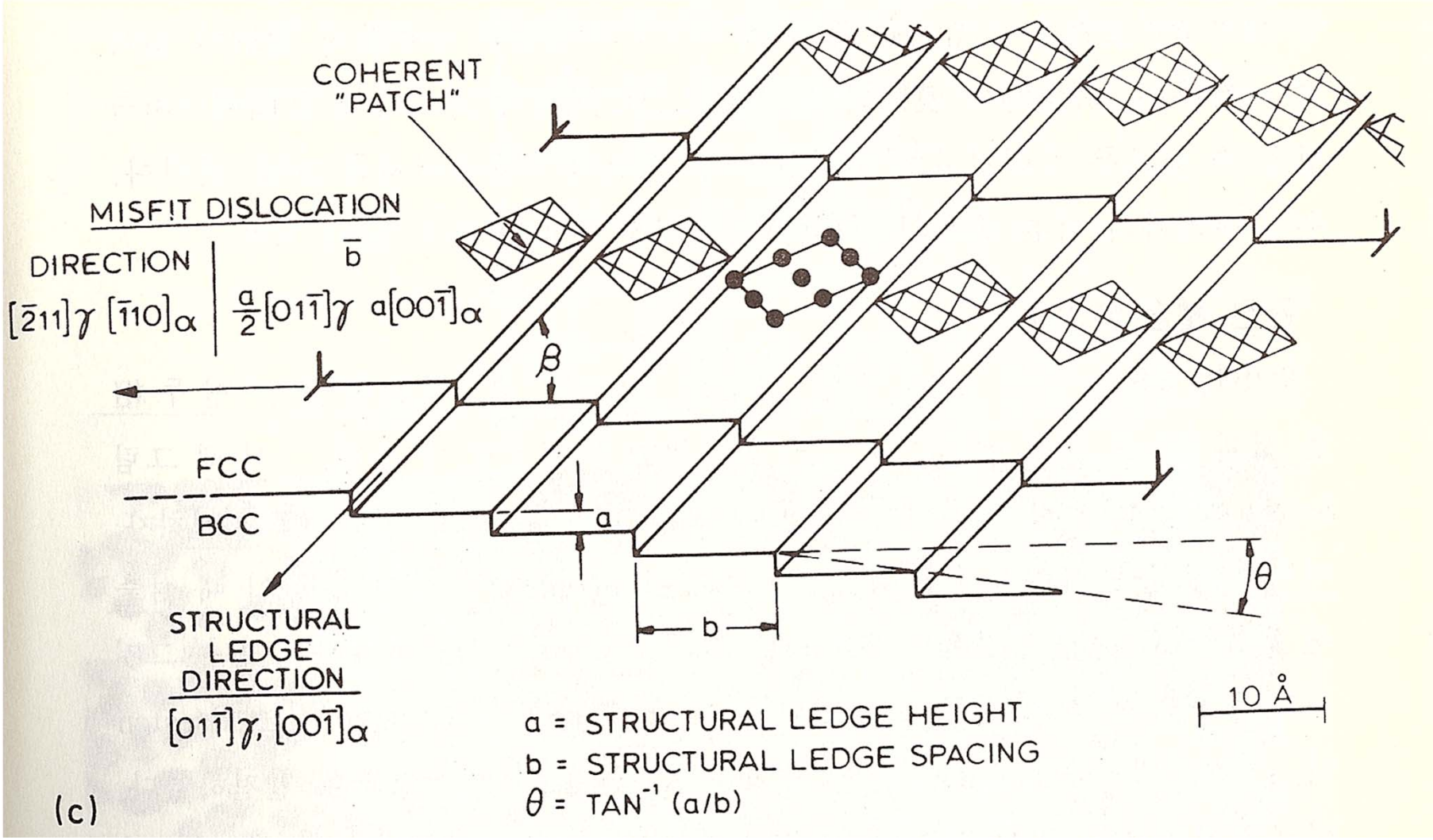

The degree of coherency can, however, be greatly increased if a macroscopically irrational interface is formed. The detailed structure of such interfaces is, however, uncertain due to their complex nature.

3.4 Interphase Interfaces in Solids

Interphase boundary - different two phases : different crystal structure
different composition

coherent, **Perfect atomic matching at interface**

γ **(coherent) =** γ_{ch} γ **(coherent) ~ 200 mJM^{-2}**

semicoherent $\gamma(semicoherent) = \gamma_{ch} + \gamma_{st}$

γ_{st} → due to structural distortions
caused by the misfit dislocations

γ**(semicoherent) ~ 200~500 mJM^{-2}**

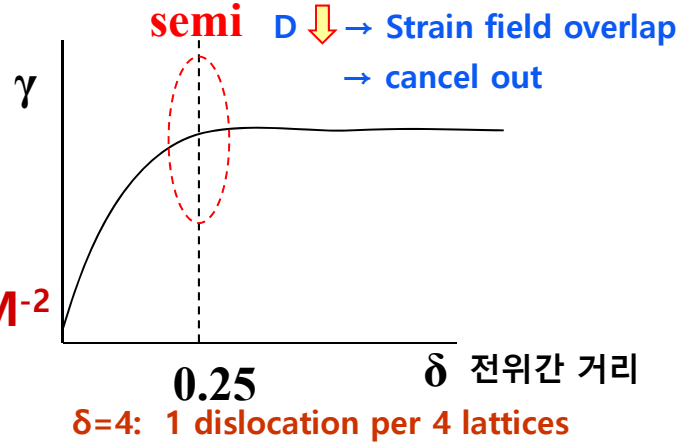

incoherent

1) δ > 0.25 No possibility of good matching across the interface

2) different crystal structure (in general)

γ **(incoherent) ~ 500~1000 mJM^{-2}**

Complex Semicoherent Interfaces

Nishiyama-Wasserman (N-W) Relationship **Kurdjumov-Sachs (K-S) Relationships**

(The only difference between these two is a rotation in the closest-packed planes of 5.26°.)

The degree of coherency can, however, be greatly increased if a macroscopically irrational interface is formed.

Q: How is the second-phase shape determined?

If misfit is small,
Equilibrium shape of a coherent precipitate or zone **can only be predicted from the "γ-plot"**

$$\sum A_i \gamma_i$$

⇒ Misfit

$$\sum A_i \gamma_i + \Delta G_S = minimum$$

"γ-plot" + "Elastic strain energy"

Lowest total interfacial free energy
by optimizing the shape of the precipitate and its orientation relationship

Fully coherent precipitates

γ_{ch} ⇒ γ_{ch} + *Lattice misfit* ⇒ γ_{ch} + $Volume\ Misfit\ \ \Delta = \frac{\Delta V}{V}$

different composition — Coherency strain energy — **Incoherent inclusions**: Chemical and structural interfacial E

(a) Precipitate shapes : $\sum A_i \gamma_i$ ⇩

(b) Calculation of misfit strain energy

3.4.2 Second-Phase Shape: Interfacial Energy Effects

How is the second-phase shape determined? $\sum A_i \gamma_i = minimum$

Lowest total interfacial free energy
by optimizing the shape of the precipitate and its orientation relationship

A. Fully Coherent Precipitates (G.P. Zone)

- If α, β have the same structure & a similar lattice parameter
- Happens during early stage of many precipitation hardening
- Good match ⇨ can have any shape ⇨ spherical

A zone with no misfit

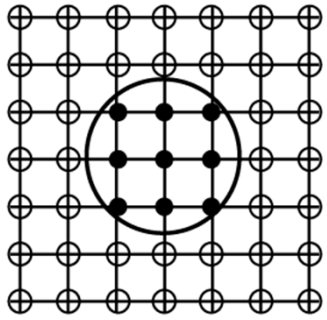

(a)

GP(Guinier- Preston) Zone in Al – Ag Alloys

$$\varepsilon_a = \frac{r_A - r_B}{r_A} = 0.7\%$$

→ negligible contribution to the total free energy

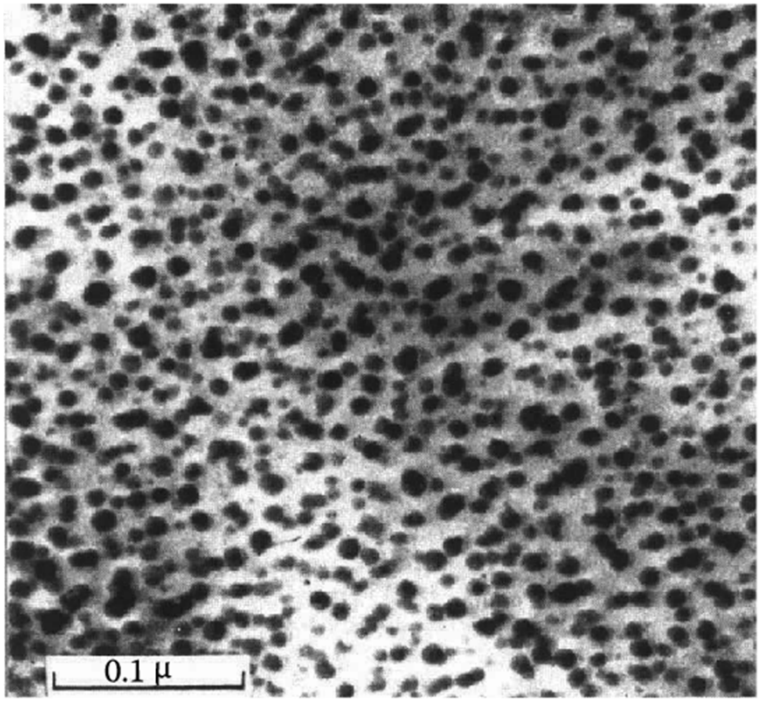

(b) Ag-rich GP zones (Dia. ~10 nm) in Al-4at% Ag alloy

B. Partially Coherent Precipitates

- α, β have different structure and one plane which provide close match

- **Coherent or Semi-coherent in one Plane;**
  Disc Shape (also plate, lath, needle-like shapes are possible)

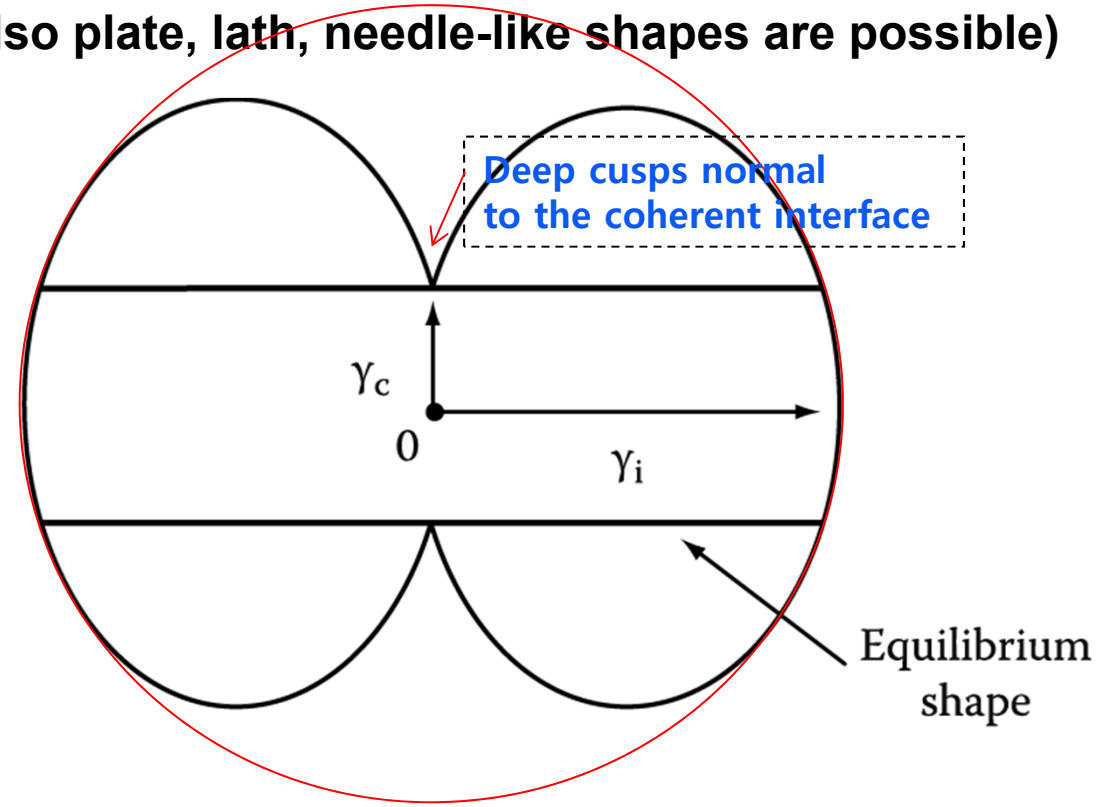

Fig. 3.40 A section through a **γ-plot** for a precipitate showing one coherent or semi-coherent interface, together with the equilibrium shape (a disc).

Precipitate shapes observed in practice
~ not equilibrium shape through a γ-plot
why? 1) misfit strain E effects ~ ignored.
2) different growth rates depending on directions

hcp γ′ Precipitates in Al – 4%Ag Alloys → plate

Semicoherent broad face parallel to the $\{111\}_\alpha$ matrix planes

(usual hcp/fcc orientation relationship)

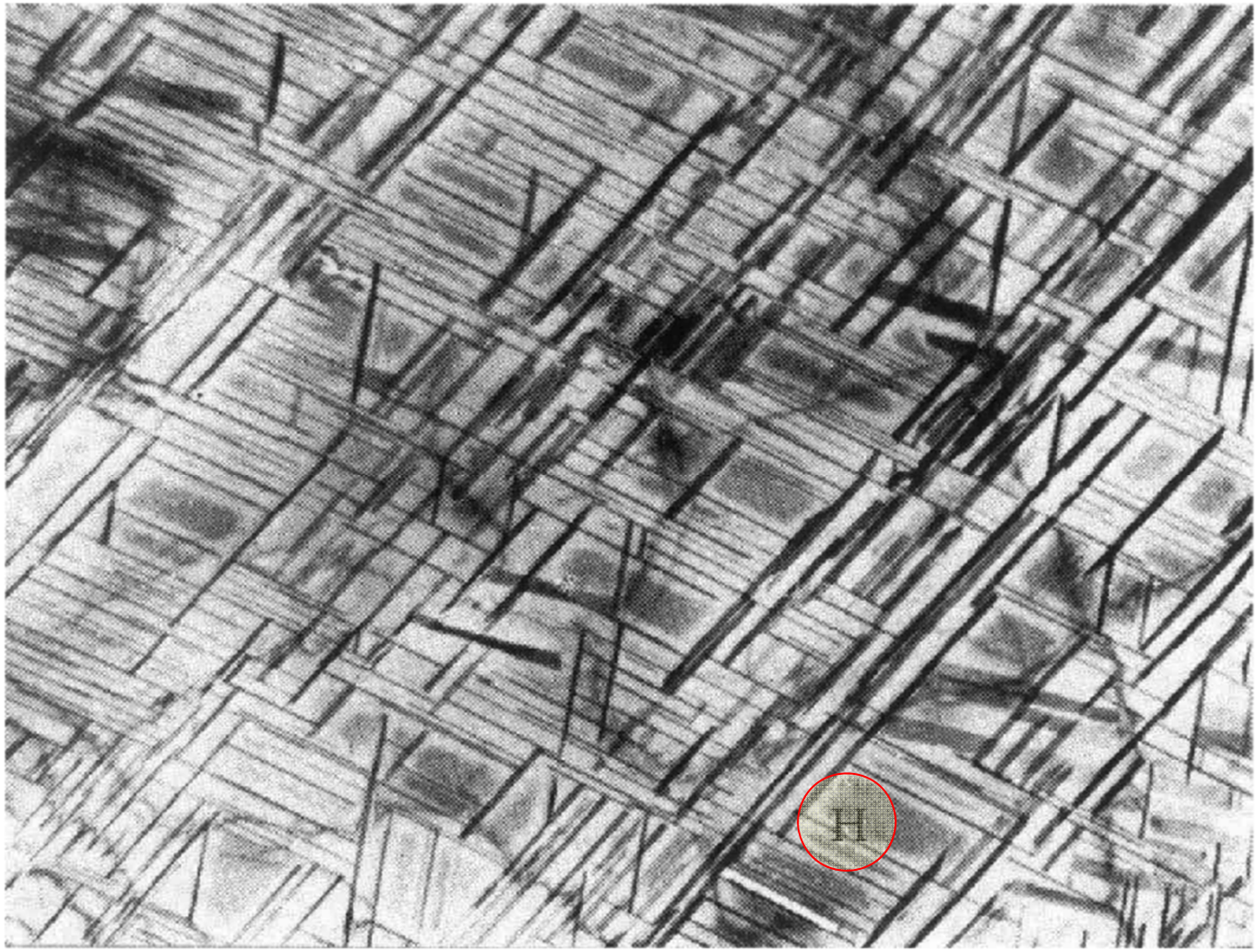

Fig. 3. 42 Electron micrograph showing the Widmanstatten morphology of γ' precipitates in an Al-4 atomic % Ag alloy. GP zones can be seen between the γ' e.g. at H (x 7000).

C. Incoherent precipitates

- when α, β have completely different structure ⇨ Incoherent interfaces
  or When the two lattices are in a random orientation
- Interface energy is high for all plane ⇨ spherical shape
  with smoothly curved interface
- Polyhedral shapes: certain crystallographic planes of the inclusion lie at cusps in the γ-plot

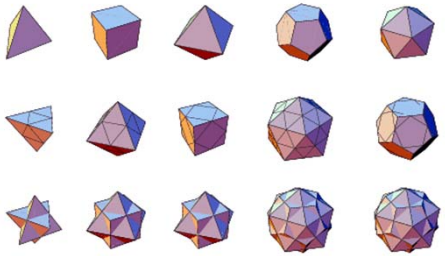

θ phase in $Al-Cu$ alloys (Al_2Cu)

Q: Example of Second-Phase Shape

precipitates from solid solution in Al-Cu alloys

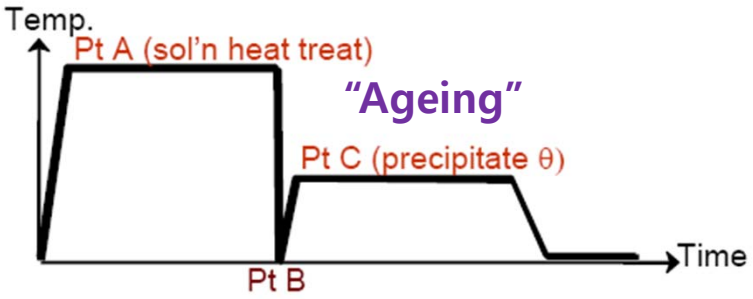

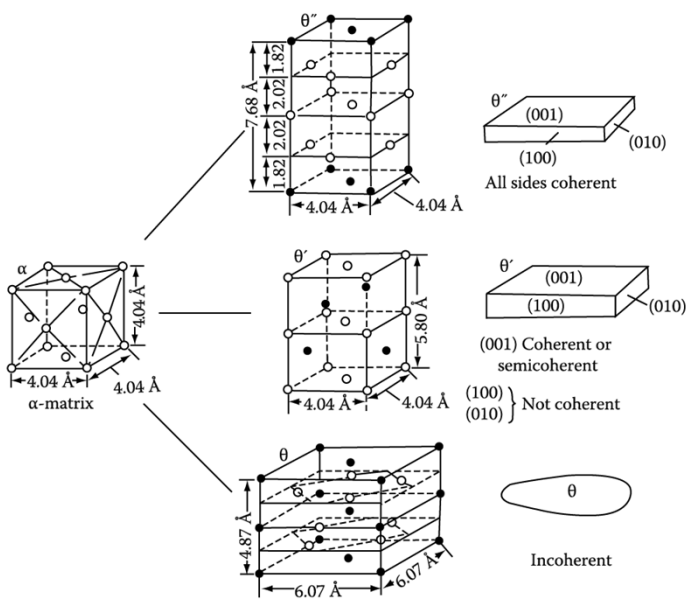

G.P. Zone

⇩

θ", all coherent

⇩

θ', partially coherent

⇩

θ, incoherent

Precipitation Hardening

- Ex: Al-Cu system
- Procedure:

- *Pt A: solution heat treat (get a solid solution)*
- *Pt B: quench to room temp.*
- *Pt C: reheat to nucleate small θ crystals within α crystals.*

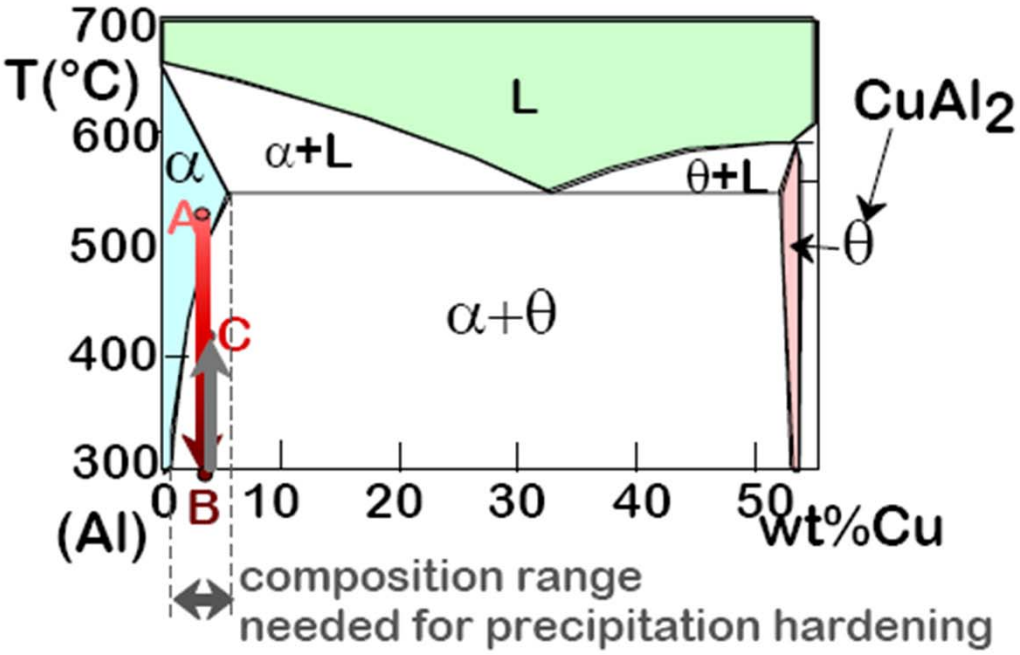

$\alpha + \theta \rightarrow$ Heat (~550°C) $\rightarrow$ Quench (0°C) $\rightarrow \alpha$ (ssss) $\rightarrow$ Heat/age (~150°C) $\alpha + \theta_{ppt}$

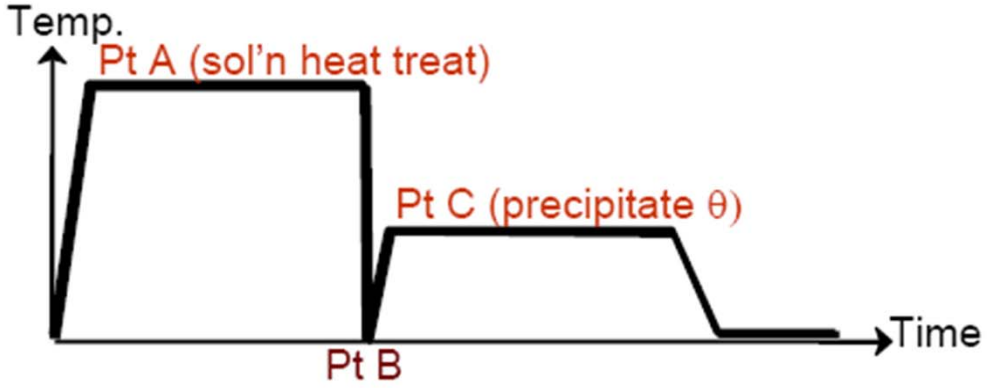

Al-Cu ppt structures

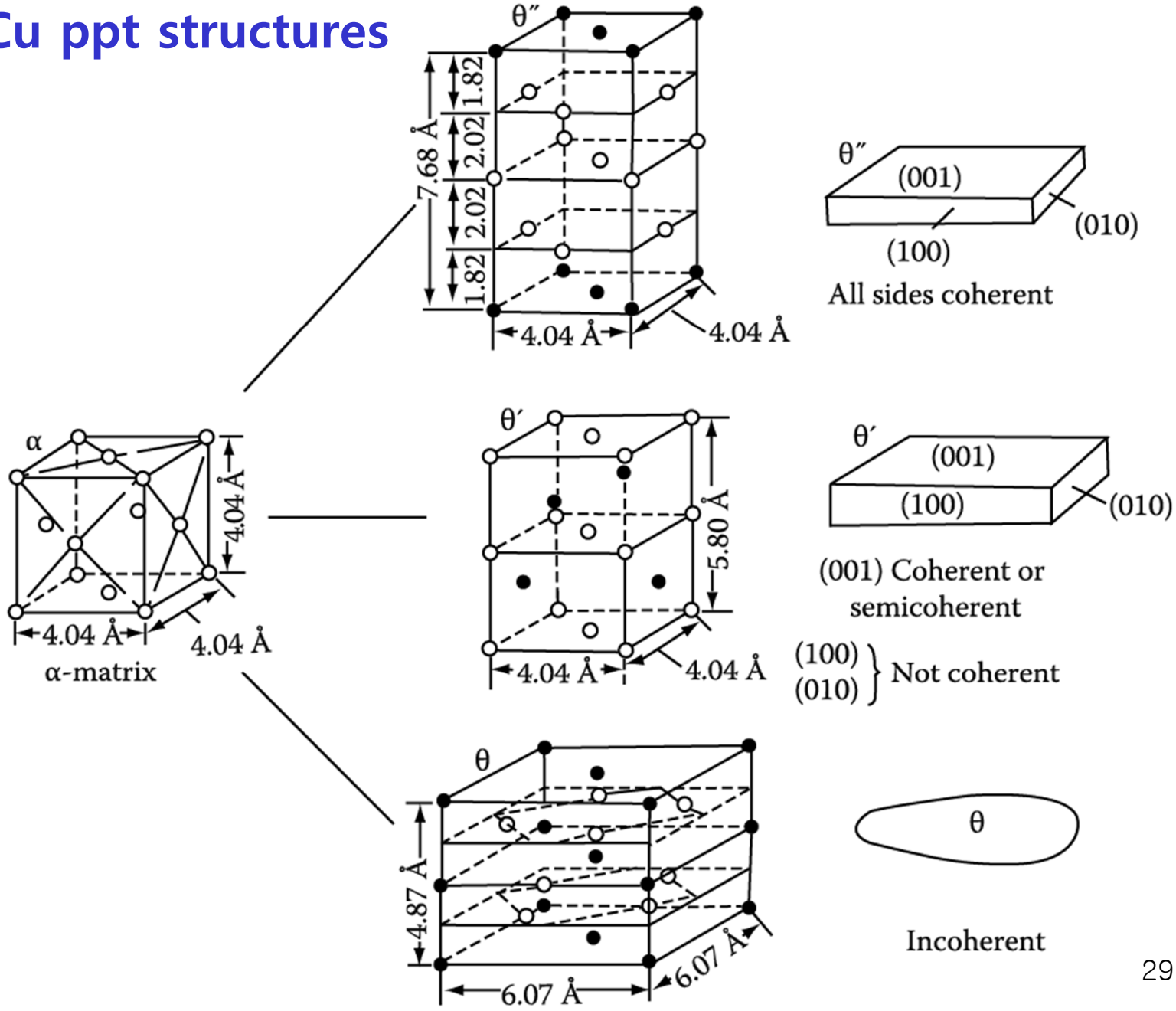

Al-Cu ppt structures

GP zone structure

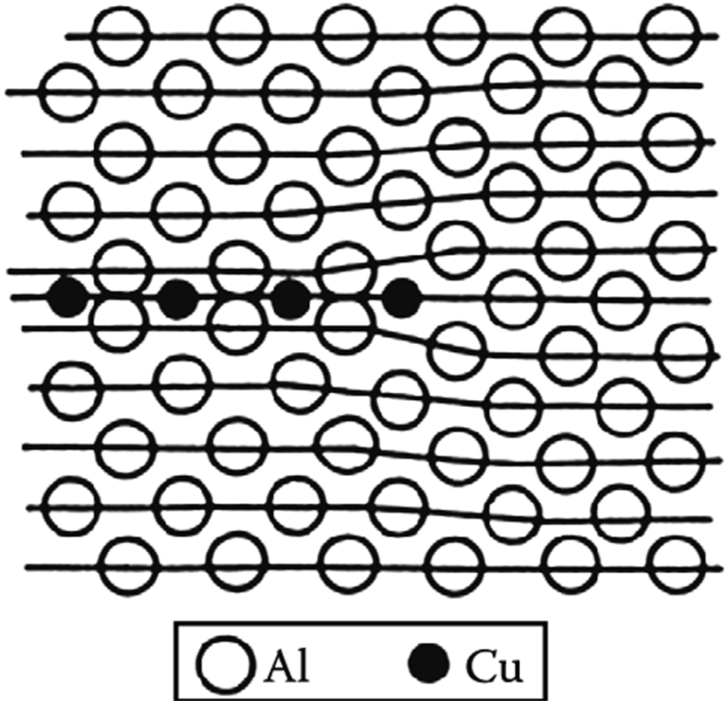

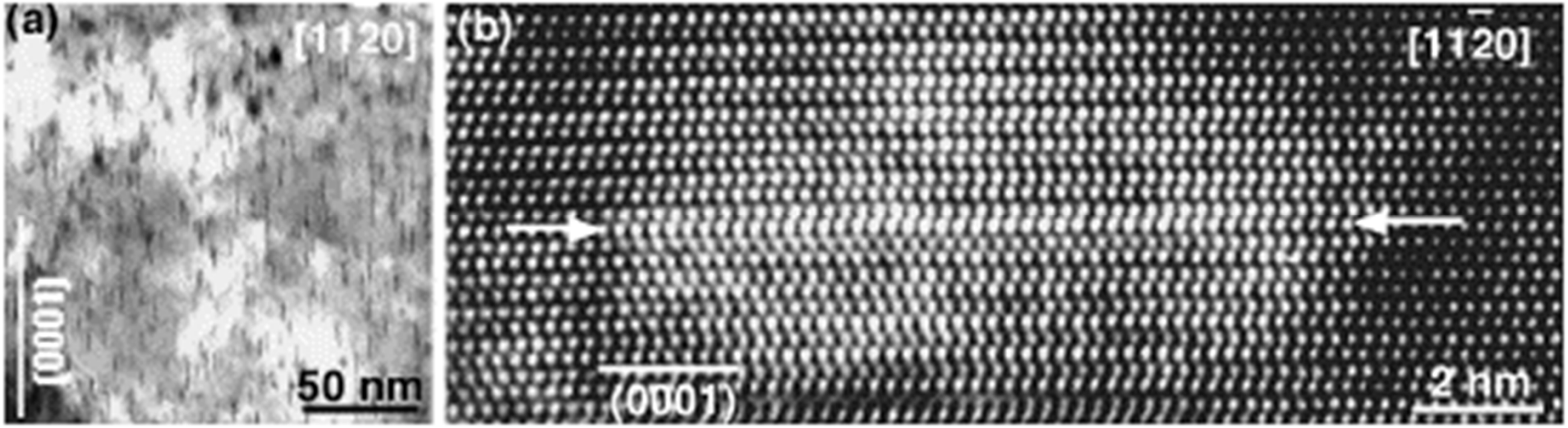

(a) Bright-field TEM image showing G.P. zones, and (b) HRTEM image of a G.P. zone formed on a single $(0\ 0\ 0\ 1)_\alpha$ plane. Electron beam is parallel to in both (a) and (b).

θ' Phase Al – Cu Alloys

Semicoherent broad face parallel to the {100}$_\alpha$ matrix planes (habit plane)

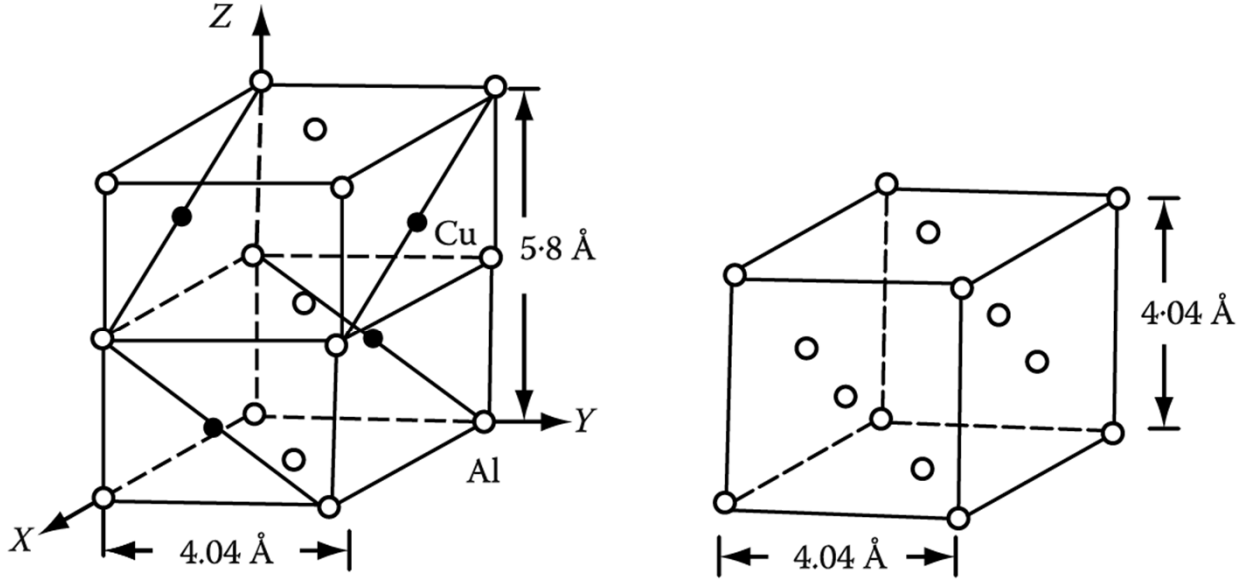

(a) The unit cell of the Θ′ precipitate in Al-Cu alloys (b) The unit cell of the matrix

Orientation relationship between α and θ'

$$(001)_{\theta'} \;//\; (001)_{\alpha} \qquad [100]_{\theta'} \;//\; [100]_{\alpha}$$

→ Cubic symmetry of the Al-rich matrix (α) ~
many possible orientations for the precipitate plates within any given grain

S phase in Al-Cu-Mg alloys ; Lath shape

β' phase in Al-Mg-Si alloys ; Needle shape

} **Widmanstätten morphology**

θ phase in $Al-Cu$ alloys (Al_2Cu)

- **Polyhedral shapes:** certain crystallographic planes of the inclusion lie at cusps in the γ-plot

5.5.4. Age Hardening

Transition phase precipitation → great improvement in the mechanical properties
Coherent precipitates → highly strained matrix → dislocations~forced during deformation

Hardness vs. Time by Ageing

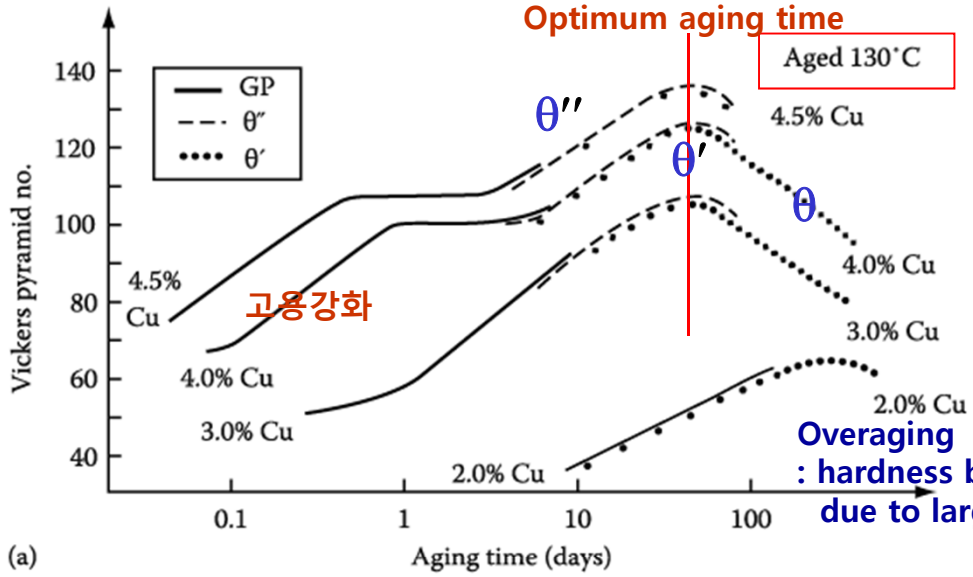

Maximum hardness~ largest fraction of θ″ (coherent precipitates)

Ageing at 130°C produces higher maximum hardness than ageing at 190°C.

At 130°C, however, it takes too a long time.

Overaging
: hardness begins to decrease due to large spacing between precipitates

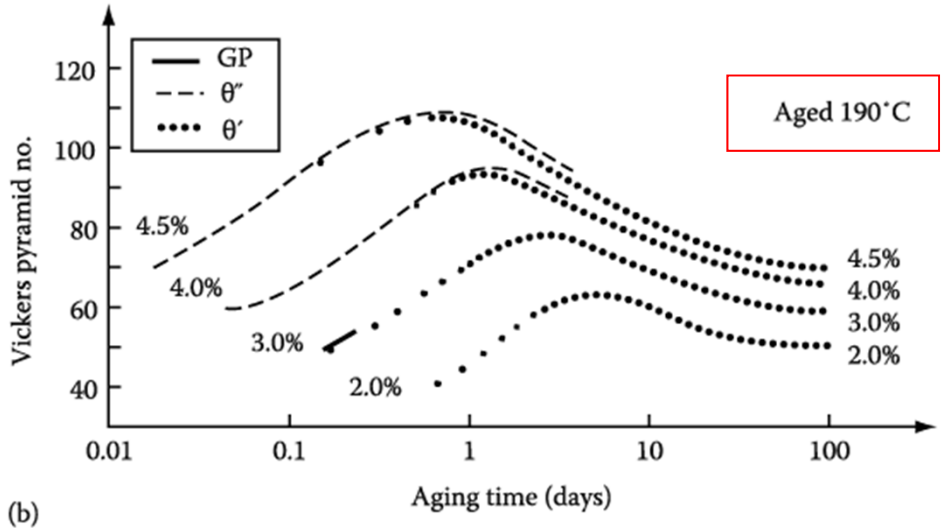

How can you get the high hardness for the relatively short ageing time?

Double ageing treatment
first below the GP zone solvus → fine dispersion of GP zones then ageing at higher T.

Finer precipitate distribution

Fig. 5. 37 Hardness vs. time for various Al-Cu alloys at (a) 130 ℃ (b) 190 ℃

Precipitates on Grain Boundaries

Formation of a second-phase particle at the interfaces with two differently oriented grains

1) incoherent interfaces with both grains

2) a coherent or semi-coherent interface with one grain and an incoherent interface with the other,

3) coherent or semi-coherent interface with both grains

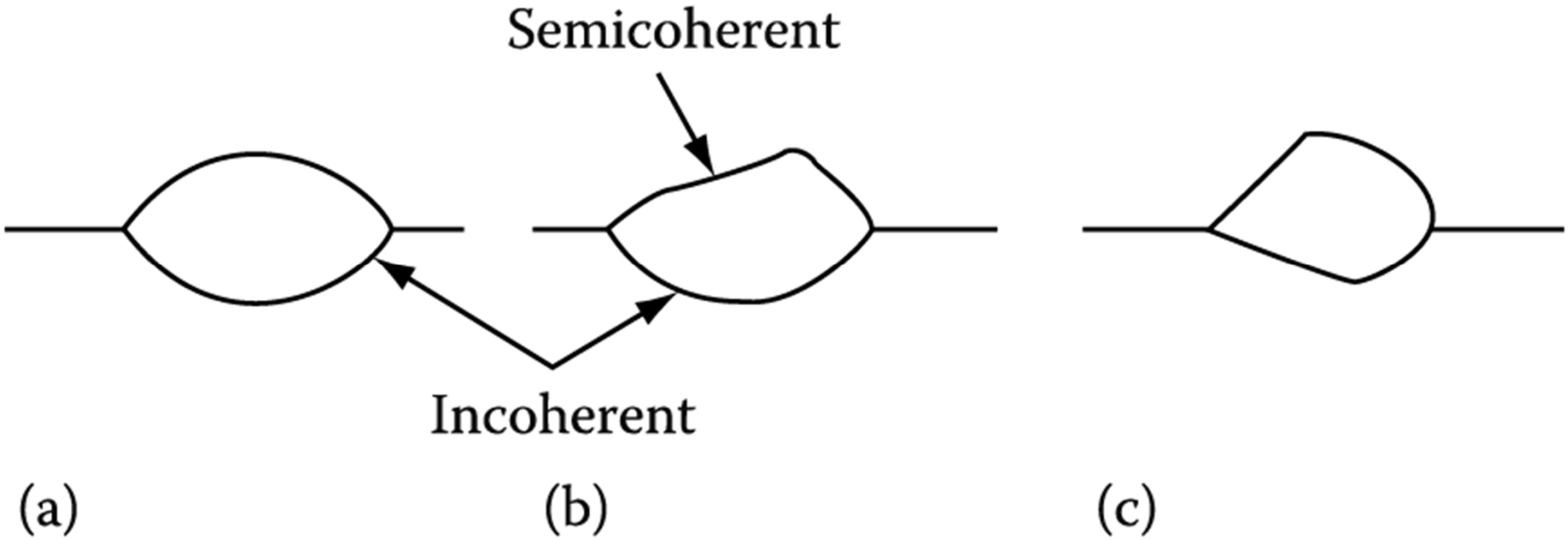

Fig. 3. 45 Possible morphologies for grain boundary precipitates. Incoherent interfaces smoothly curved. Coherent or semicoherent interface plannar.

Precipitates on Grain Boundaries

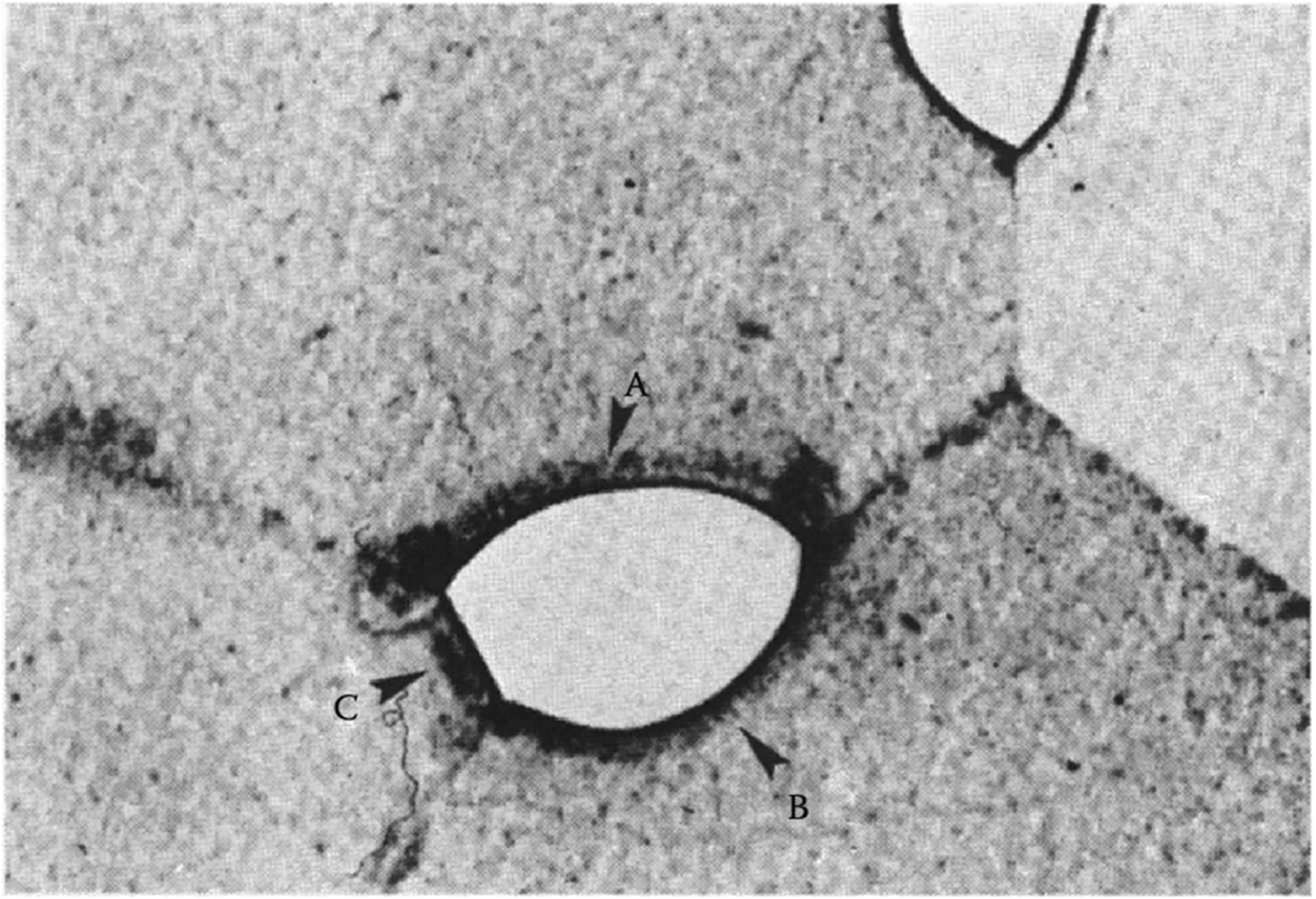

Fig. 3. 46 An α precipitate at a grain boundary triple point in an α – β Cu-In alloy. Interfaces A and B are incoherent while C is semicoherent (x 310).

A, B; Incoherent, C; Semi-coherent or coherent

3.4 Interphase Interfaces in Solids (α/β)

$$\sum A_i \gamma_i + \Delta G_S = minimum$$

1) Interphase boundary - different two phases : different crystal structure
different composition

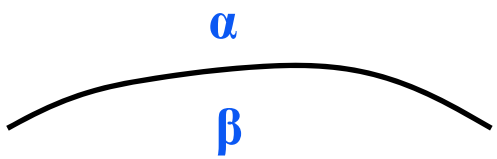

- Coherent/ Semicoherent/ Incoherent
- Complex Semicoherent

Fully coherent precipitates

γ_{ch} ⇨ γ_{ch} + *Lattice misfit* ⇨ γ_{ch} + $Volume\ Misfit\quad \Delta = \frac{\Delta V}{V}$

different composition — Coherency strain energy — Chemical and structural interfacial E

Incoherent inclusions

2) Second-Phase Shape: precipitate from solid solution in Al-Cu alloys

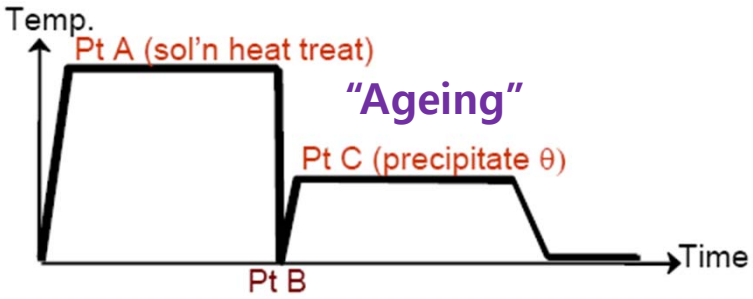

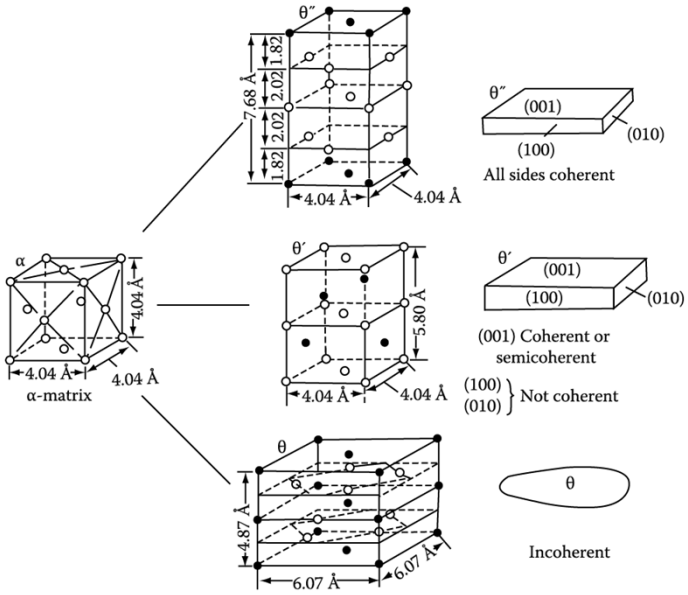

- **G.P. Zone**
- ⇩
- **θ", all coherent**
- ⇩
- **θ', partially coherent**
- ⇩
- **θ, incoherent**

Q: How is the second-phase shape determined?

$$\sum A_i \gamma_i + \Delta G_S = minimum$$

γ – plot + misfit strain E

Lowest total interfacial free energy
by optimizing the shape of the precipitate and its orientation relationship

Fully coherent precipitates

γ_{ch} ⇨ γ_{ch} + ***Lattice misfit*** ⇨ γ_{ch} + $Volume\ Misfit\quad \Delta = \frac{\Delta V}{V}$

different composition — Coherency strain energy — **Incoherent inclusions**: Chemical and structural interfacial E

(a) Precipitate shapes

(b) Calculation of misfit strain energy

3.4.3. Second-Phase Shape: Misfit Strain Effects

If misfit is small,
Equilibrium shape of a coherent precipitate or zone can only be predicted from the "γ-plot"

$\sum A_i \gamma_i$

Misfit

$$\sum A_i \gamma_i + \Delta G_S = minimum$$

"γ-plot" + "Elastic strain energy"

A. Fully Coherent Precipitates

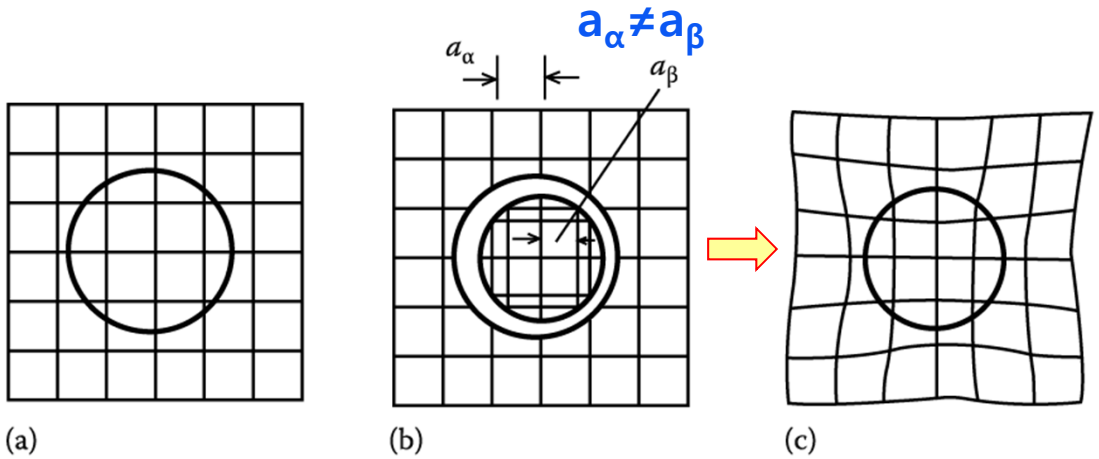

Distortion (격자변형) is pure hydrostatic, i.e., it is uniform in all directions. → new lattice parameter a_β'

Fig. 3. 47 The origin of coherency strains. The number of lattice points in the hole is conserved.

Unconstrained Misfit *Constrained Misfit*

구속되지 않은 불일치도 $\delta = \dfrac{a_\beta - a_\alpha}{a_\alpha}$ ⇨ 구속된 불일치도 $\varepsilon = \dfrac{a'_\beta - a_\alpha}{a_\alpha}$

① If $E_\beta = E_\alpha, \nu = 1/3 \rightarrow \varepsilon = \dfrac{2}{3}\delta$

Poisson's ratio

② In practice, different elastic constants $E_\beta \neq E_\alpha \rightarrow 0.5\delta \leq \varepsilon \leq \delta$

if thin disc-type precipitate,

⇨ **In situ misfit is no longer equal in all directions**

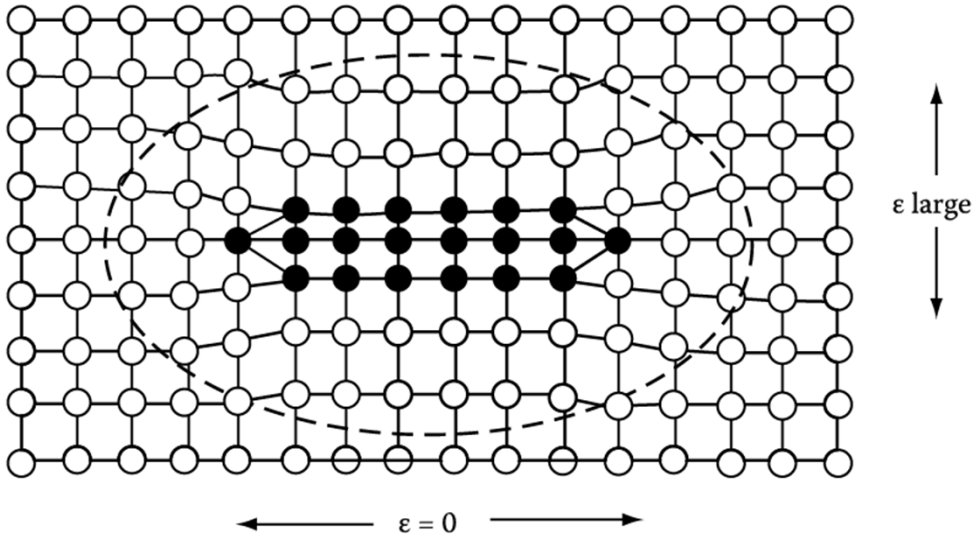

Fig. 3. 48 For a coherent thin disc there is **little misfit parallel to the plane of the disc. Maximum misfit is perpendicular to the disc. → reduction in coherency strain E**

* **Total elastic energy (ΔG_s) depends on the "shape" and "elastic properties" of both matrix and inclusion.**

Elastically Isotropic Materials & $E_\beta = E_\alpha$

$\Delta G_S = 4\mu\delta^2 \cdot V$ (If ν=1/3)

here, μ= shear modulus of the matrix,

V= volume of the unconstrained hole in the matrix

ΔGs→ independent of the shape of the precipitate

Elastically Anisotropic Materials & $E_\beta \neq E_\alpha$

ΔGs→ dependent of the shape of the precipitate

ΔG_s^{min}: if inclusion is hard→sphere/ soft→disc shape

Atom radius ($\overset{o}{A}$)	*Al* : 1.43	*Ag* : 1.44	*Zn* : 1.38	*Cu* : 1.28
Zone Misfit (δ)	–	+ 0.7 %	– 3.5 %	– 10.5 %
***GP** Zone Shape*	–	*sphere*	*sphere*	*disc*

Equilibrium shape

$\sum A_i\gamma_i + \Delta G_S = minimum$

Interfacial E effect dominant

$\delta < 5\%$

strain E effect dominant

Influence of strain E (δ =lattice misfit) on the equilibrium shape of coherent precipitation

B. Incoherent Inclusions

Lattice sites are not conserved. → no coherency strain, ΔG_S

But, misfit strain still arise if the inclusion is the wrong size.

δ (lattice misfit) → Δ (volume misfit)

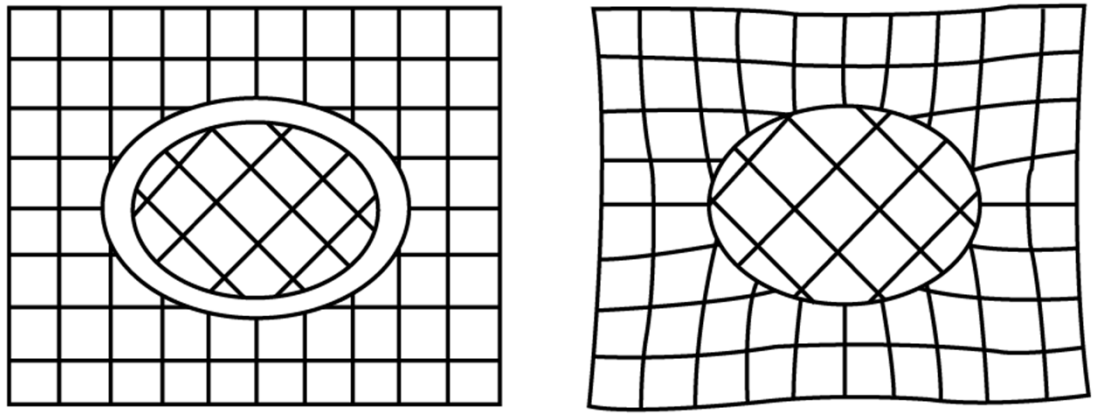

(a) (b)

#of lattice sites within the hole is not preserved for incoherent inclusion (no lattice matching)

$$\text{Volume Misfit} \quad \Delta = \frac{\Delta V}{V}$$

Ex) coherent spherical inclusion: $\Delta = 3\delta$

For spheroidal Inclusions $\dfrac{x^2}{a^2}+\dfrac{y^2}{b^2}+\dfrac{z^2}{c^2}=1$

For Elliptical Inclusions $\dfrac{x^2}{a^2}+\dfrac{y^2}{a^2}+\dfrac{z^2}{c^2}=1$

For a homogeneous incompressible inclusion in an isotropic matrix

등방성 기지내 균질 비압축성 개재물

Nabarro Eq.

$$\Delta G_S = \frac{2}{3}\mu\Delta^2 \cdot V \cdot f(c/a)$$

μ: the shear modulus of the matrix

1) The elastic strain energy is proportional to the square of the volume misfit Δ^2.

2) Shape effect for misfit strain E ~ function *f* (c/a)

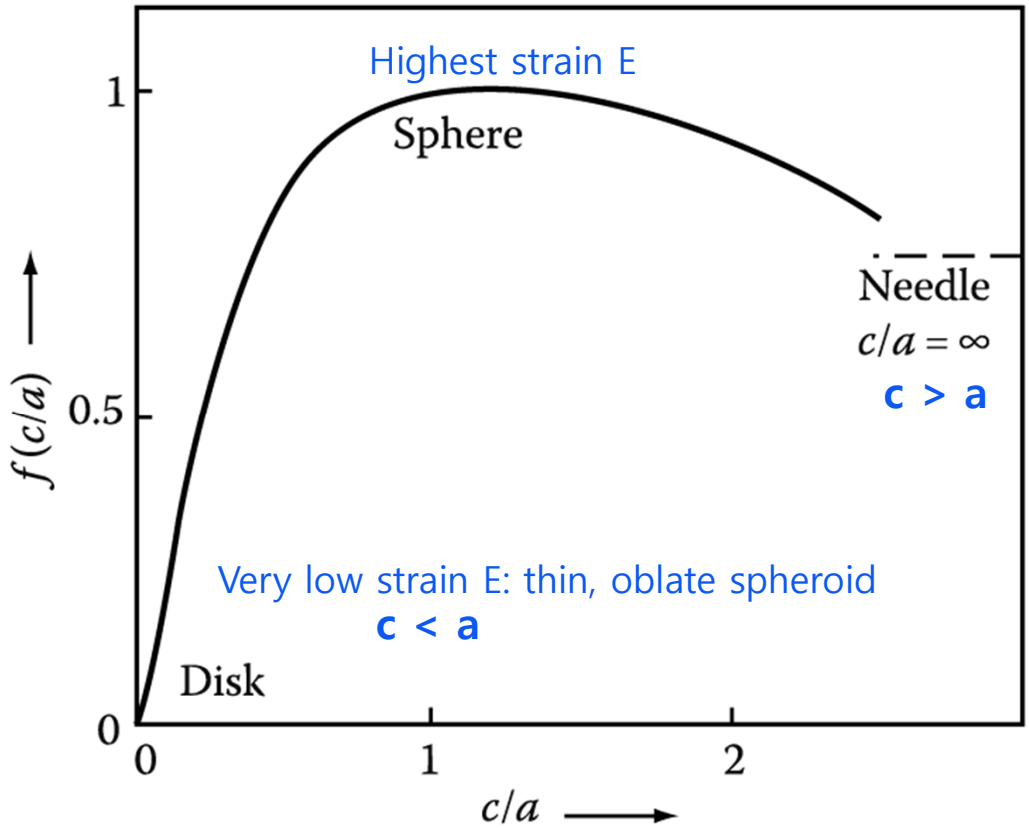

c < a

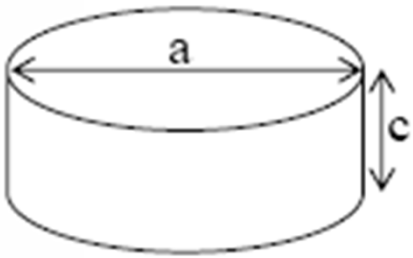

c > a

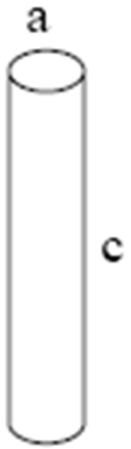

If elastic anisotropy is included, same general form for f(c/a) is preserved.

Fig. 3. 50 The variation of misfit strain energy with ellipsoid shape, f(c/a).

$$\Delta G_s = \frac{2}{3}\mu \Delta^2 \cdot V \cdot f(c/a) \qquad \Delta = \frac{V_\beta - V_\alpha}{V_\alpha} \approx 3\delta \text{ for sphere}, \quad \neq 3\delta \text{ for disc or needle}$$

Elastic strain E

Precipitate shape effect

* Equil. Shape of an incoherent inclusion: an oblate spheroid with c/a value that balances the opposing effects of interfacial E and strain E

(here, Δ ~ small → Interfacial E dominant → roughly spherical inclusion)

C. Plate-like precipitates

Misfit across the broad faces → large coherency strains parallel to the plate

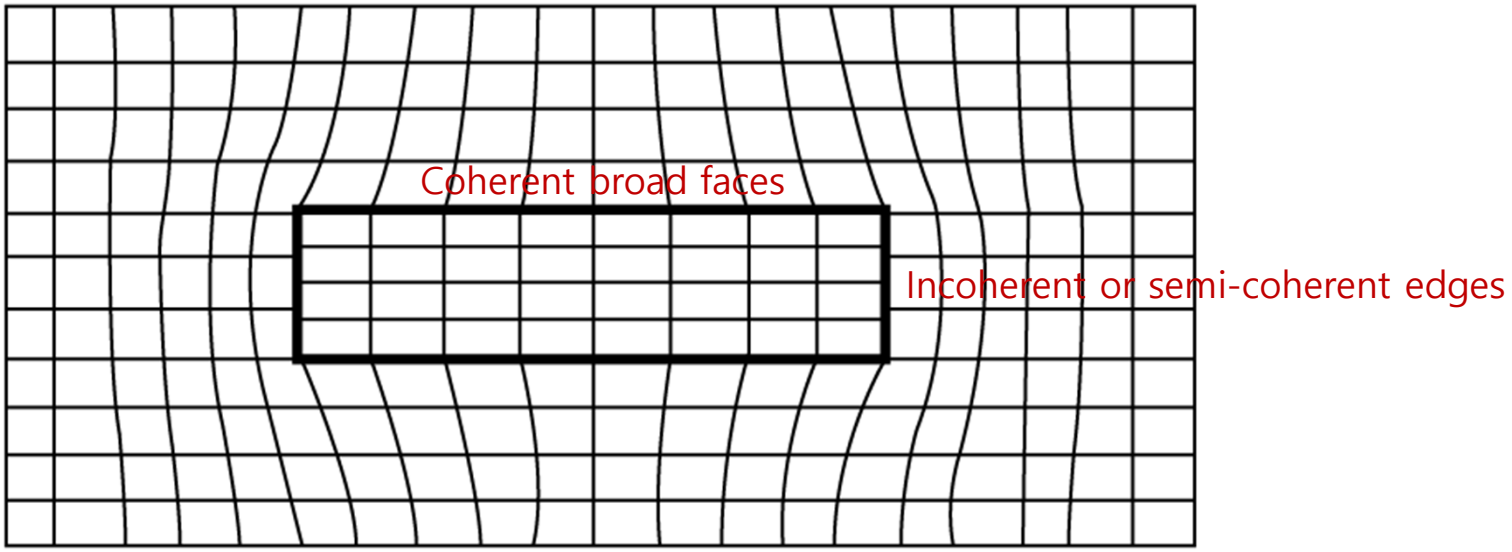

In situ misfit across the broad faces increases with increasing plate thickness

→ **greater strains the matrix and higher shear stresses at the corners of the plates**

→ **energetically favorable for the broad faces to become semi-coherent**

→ **the precipitate behaves as an incoherent inclusion with comparatively little misfit strain E, ex) θ' phase in Al-Cu alloy**

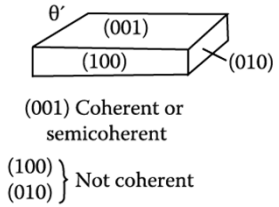

Q: Which state produces the lowest total E for a spherical precipitate?

"Coherency loss"

If a coherent precipitate grows, during aging for example, It should lose coherency when it exceeds r_{crit}.

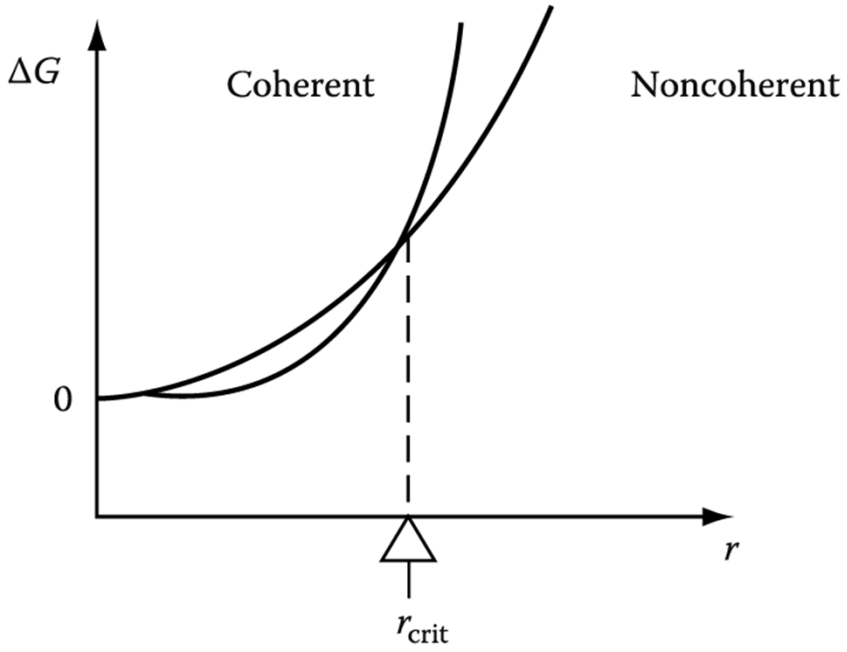

Coherency Loss

- Precipitates with coherent interfaces=low interfacial E + coherency strain E
- Precipitates with non-coherent interfaces=higher interfacial E

If a coherent precipitate grows, it should lose coherency to maintain minimum interfacial free E.

$$\Delta G(coherent) = 4\mu\delta^2 \cdot \frac{4}{3}\pi r^3 + 4\pi r^2 \cdot \gamma_{ch} \quad \Leftrightarrow \quad \Delta G(non-coherent) = 4\pi r^2 \cdot (\gamma_{ch} + \gamma_{st})$$

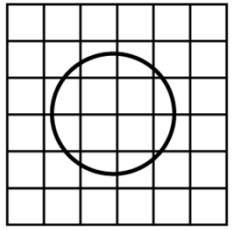

Coherency strain energy
Eq. 3.39

Chemical interfacial E

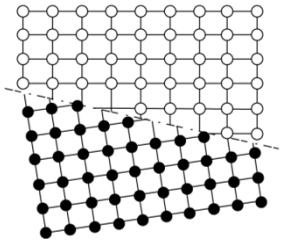

Chemical and structural interfacial E

$$\frac{4}{3}\pi r^3\left(4\pi\mu\delta^2\right) + 4\pi r^2\left(\gamma_{ch}\right) = 4\pi r^2\left(\gamma_{st} + \gamma_{ch}\right)$$

coherent ΔG_s-relaxed

$$\therefore r_{crit} = \frac{3\cdot\gamma_{st}}{4\mu\delta^2}$$

$$for\ small\ \delta,\quad \gamma_{st} \propto \delta$$

(semi-coherent interface)

$$\approx \frac{1}{\delta}$$ ($\delta = (d_\beta - d_\alpha)/ d_\alpha$: misfit)

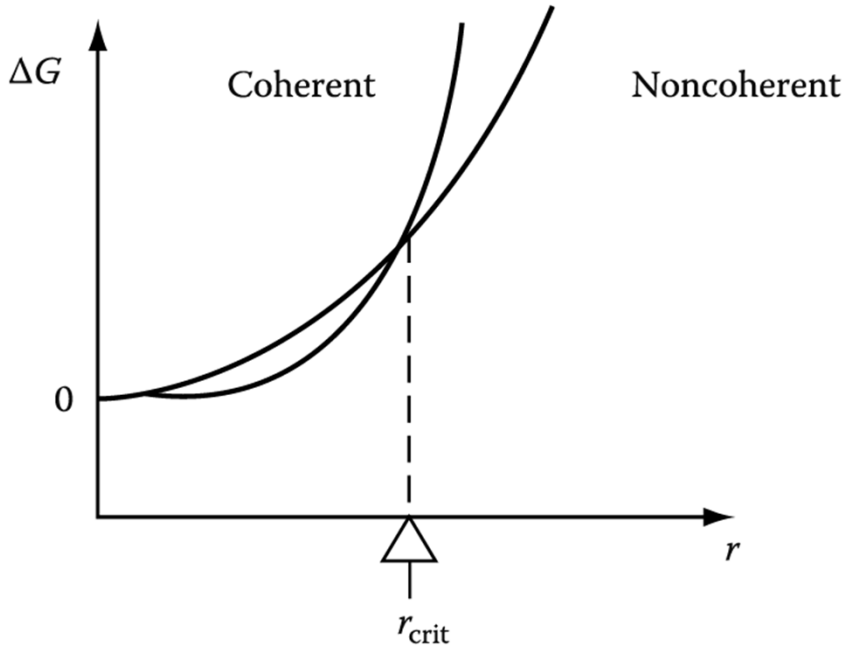

Fig. 3. 52 The total energy of matrix + precipitate vs. precipitate radius for spherical coherent and non-coherent (semicoherent of incoherent) precipitates.

If a coherent precipitate grows, during aging for example,
It should lose coherency when it exceeds r_{crit}.

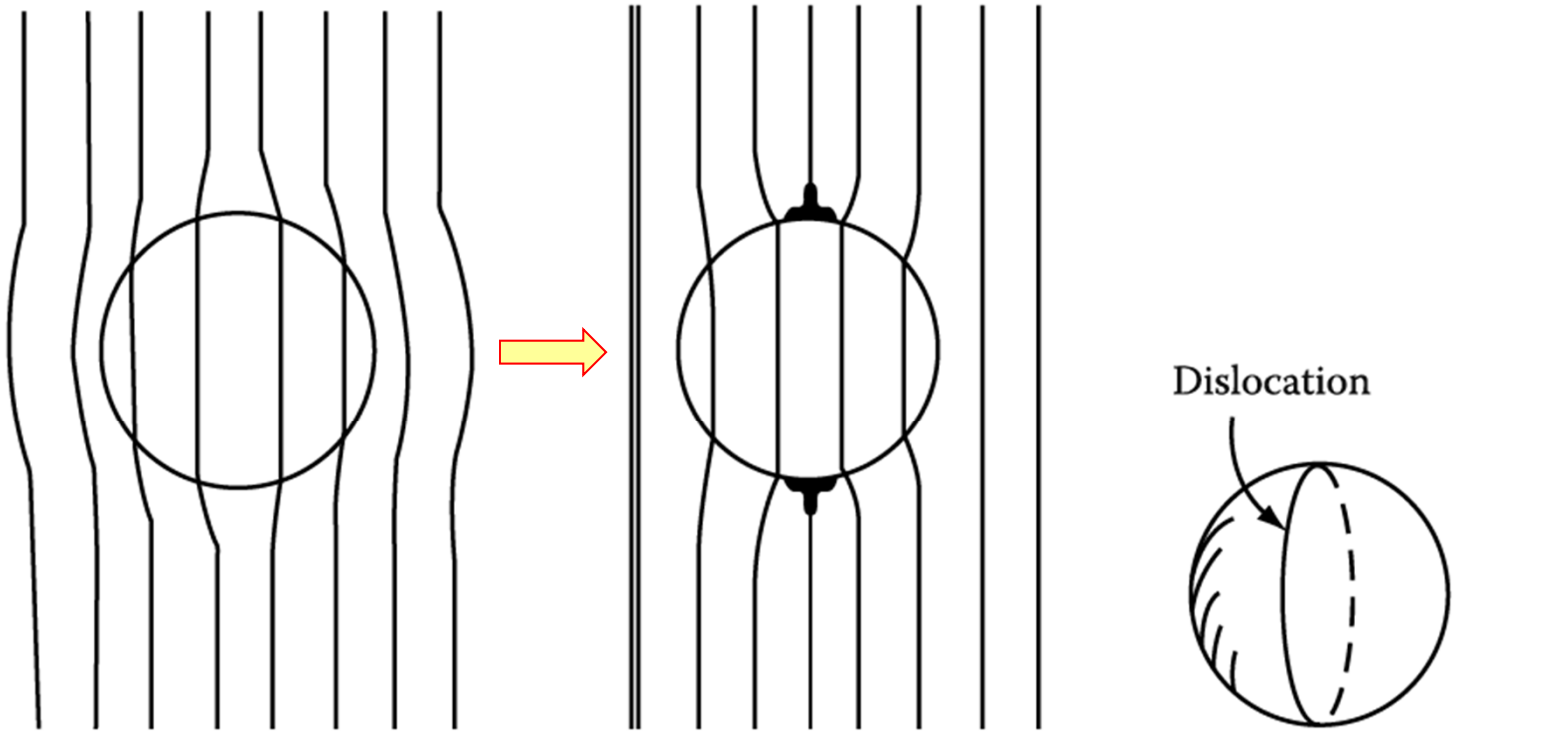

(a) Coherent with strain E (b) Coherency strain replace by dislocation loop. (c) Precipitate with dislocation

Fig. 3.53. Coherency loss for a spherical precipitate

In practice, this phenomena can be rather difficult to achieve.
→ Coherent precipitates are often found with sizes much larger than r_{crit}.

"Mechanisms for coherency loss": all require the precipitate to reach a larger size than r_{crit}

1) spherical precipitate

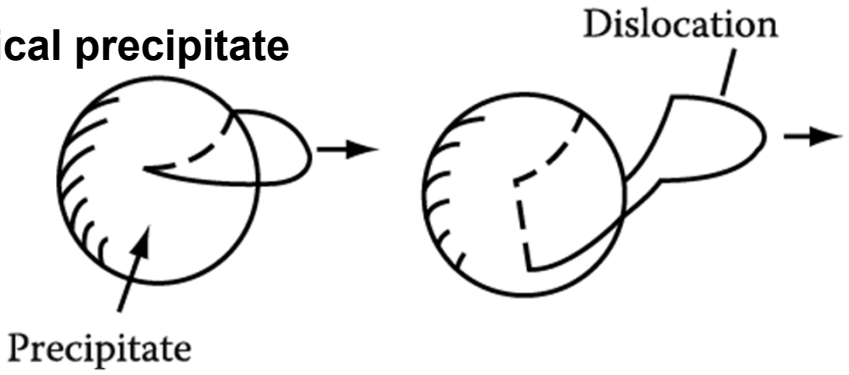

* Punching stress (P_s) ~ independent of size, but $P_s \propto$ constrained misfit, ε ($>\varepsilon_{crit}\sim0.05$), → "precipitates with a smaller ε cannot lose coherency by (a), no matter how large."

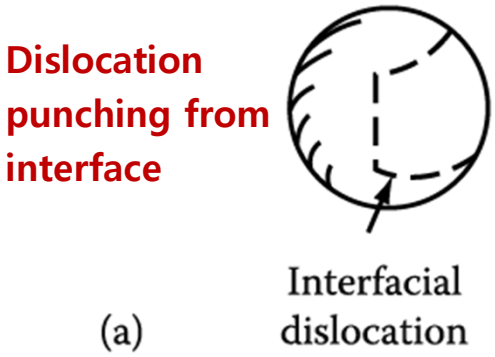

Dislocation punching from interface

requires the stresses at the interface to exceed the theoretical strength of the matrix

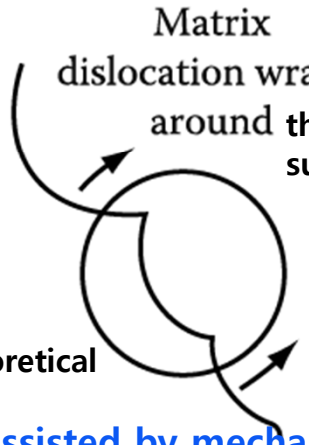

the precipitate with a suitable Burgers vector

assisted by mechanical deformation

(b) Capture of matrix dislocation

2) Plate precipitate

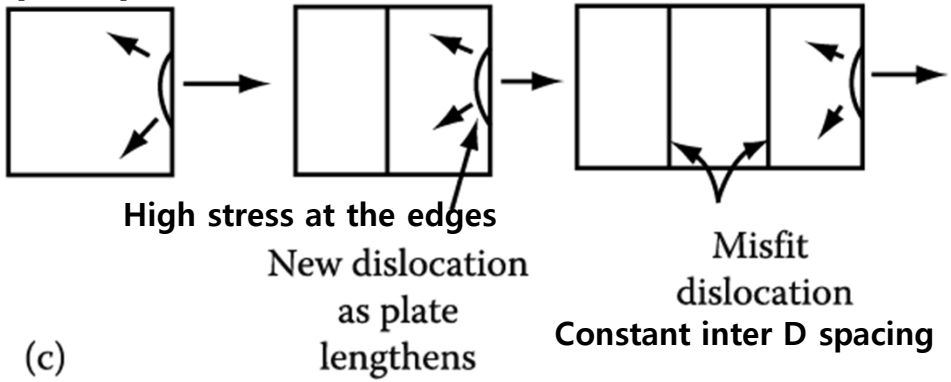

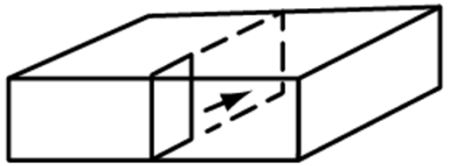

Prismatic dislocation loop

Nucleation of D loops within the precipitate

Nucleation of dislocation at the edge → maintain a roughly constant inter-dislocation spacing during plate lengthening

(d) Vacancies can be attracted to coherent interfaces and 'condense' to form a prismatic dislocation loop which can expand across the precipitate